Table 2.7 Logistic regressions of total hepatic lesion scores in mice exposed perinatally to BPA. Risk ratios for total, co-occurring hepatic lesions in mice exposed perinatally to control diet or to one of three doses of BPA (50 ng/kg diet, 50 μg/kg diet, or 50 mg/kg diet) were generated using logistic regression models, adjusted for clustering of mice within litters using Generalized Estimating Equations (GEE).

Toxic hepatic lesion score model	Dose (per kg diet)	Risk ratio	Lower limit	Upper limit	Parameter p-value	p for trend
			95% confidence interval			
Summary score (all lesions)	Control	Reference				
	50 ng BPA	1.30	0.83	2.06	0.558	
	50 μg BPA	1.56	1.19	2.04	0.097	
	50 mg BPA	1.76	1.28	2.41	0.075	
						0.086
Summary score (less steatosis)	Control	Reference				
	50 ng BPA	1.40	0.85	2.30	0.496	
	50 μg BPA	1.69	1.24	2.28	0.073	
	50 mg BPA	1.98	1.40	2.79	*0.046*	
						0.054
Summary score (less steatosis and inflammation)	Control	Reference				
	50 ng BPA	1.85	1.03	3.30	0.293	
	50 μg BPA	2.41	1.62	3.58	*0.026*	
	50 mg BPA	2.70	1.74	4.18	*0.024*	
						0.023

*p-values <0.05 are shown in italics †Total summary scores included the following ten lesions: hepatic adenoma; hepatocellular carcinoma; hyperplastic nodule; oval cell hyperplasia; Kupffer cell hyperplasia; multinucleated hepatocytes; steatosis; inflammation; hepatocyte hypertrophy; lipofuscin deposition. No animal presented with greater than eight (8) lesions. Two additional summary scores were computed, excluding steatosis or excluding both steatosis and inflammation, to avoid masking true effects with highly prevalent background lesions.

Table 2.8 SNP genotyping shows mice from this study are 93% C57BL/6J genome-wide, and >99% C57BL/6J on chromosome 1, including the *Hcs7* (*Hepatocellular carcinogenicity locus 7*) locus. Three mice (one yellow *A*^{vy}*/a* , one black *a/a* and one C57BL/6J) were genotyped for 74,830 SNPs scattered throughout the genome. Non-C57BL/6J SNPs occur mostly in blocks and may represent low-level introgression from another strain, likely C3H.

Chromosome	Total # SNPs	# Assayable	# SNPs unique to (*A*^{vy}) yellow	# SNPs not C57BL/6J-like	% C57BL/6J	Where is the chromosome not C57BL/6-like (possibly C3H)?
1	5464	5416	0	6**	99.89	
2	5470	5432	54*	161	97.04	Agouti locus & tip
3	4458	4416	0	743	83.17	Top two-thirds
4	4408	4341	0	287	93.39	Top quarter and tip
5	4379	4346	0	188	95.67	Lower tip
6	4163	4121	0	733	82.21	Scattered throughout
7	4475	4408	0	380	91.38	Middle third
8	3818	3783	0	7	99.81	
9	3856	3823	0	1381	63.88	Scattered throughout
10	3803	3777	0	5	99.87	
11	4330	4287	0	416	90.30	3 scattered blocks
12	3514	3490	0	3	99.91	
13	3649	3621	0	2	99.94	
14	3235	3205	0	28	99.13	One small block
15	2998	2981	0	138	95.37	One block
16	2868	2849	0	2	99.93	
17	3018	2989	0	1	99.97	
18	2762	2728	0	759	72.18	Scattered on top half
19	2411	2387	0	4	99.83	
X	2378	2342	0	4	99.83	
Y	38	37	0	0	100.00	
Mitochondria	53	51	0	0	100.00	
Summary	**75548**	**74830**	**54**	**5247**	**92.99**	**Range is 63.88% to 99.97%**

*The *Agouti* (*A*^{vy}) locus is contained within the 54 SNPs on chromosome 2 that differed between yellow and black mice; this is the only region in which the *A*^{vy}*/a* and *a/a* mice differed.

†The *A*^{vy}*/a* and *a/a* mice differed from the C57BL/6J mouse at only 6 of 5416 SNPs on chromosome 1: B6_rs31362610; B6_rs3659238; B6_01-0749630; B6_rs31375526; UNC010465120; and B6_rs6341208.
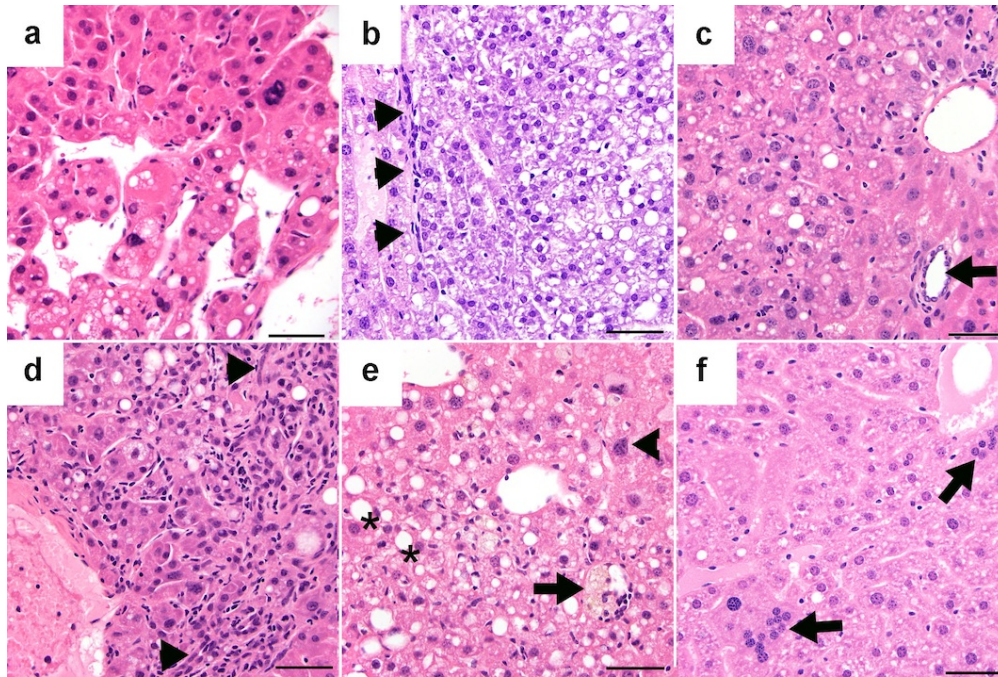
Figure 2.1 Representative photomicrographs of hepatic lesions in BPA-exposed mice. *(A)* Hepatocellular carcinoma in a female mouse exposed to 50 mg BPA/kg maternal diet. *(B)* Hepatic adenoma in a male mouse exposed to 50 mg BPA/kg maternal diet. Arrows indicate line of demarcation between neoplasm and compressed adjacent normal parenchyma. *(C)* Hyperplastic nodule in a female mouse exposed to 50 ng BPA/kg maternal diet. Arrow shows a bile duct as part of a portal triad within the lesion, indicating preservation of hepatic architecture. *(D)* Oval cell hyperplasia (arrowheads) and increased Kupffer cells within sinusoids (Kupffer cell hyperplasia) in a male mouse exposed to 50 ng BPA/kg diet. *(E)* Degenerative changes including lipofuscin accumulation (arrow), hepatocellular hypertrophy (arrowhead), and steatosis (asterisks) in a female mouse exposed to 50 ng BPA/kg diet. *(F)* Multinucleated hepatocytes (arrows) in a male mouse exposed to 50 mg BPA/kg diet. Hematoxylin and eosin. Original magnification x400. Bar 50µm.
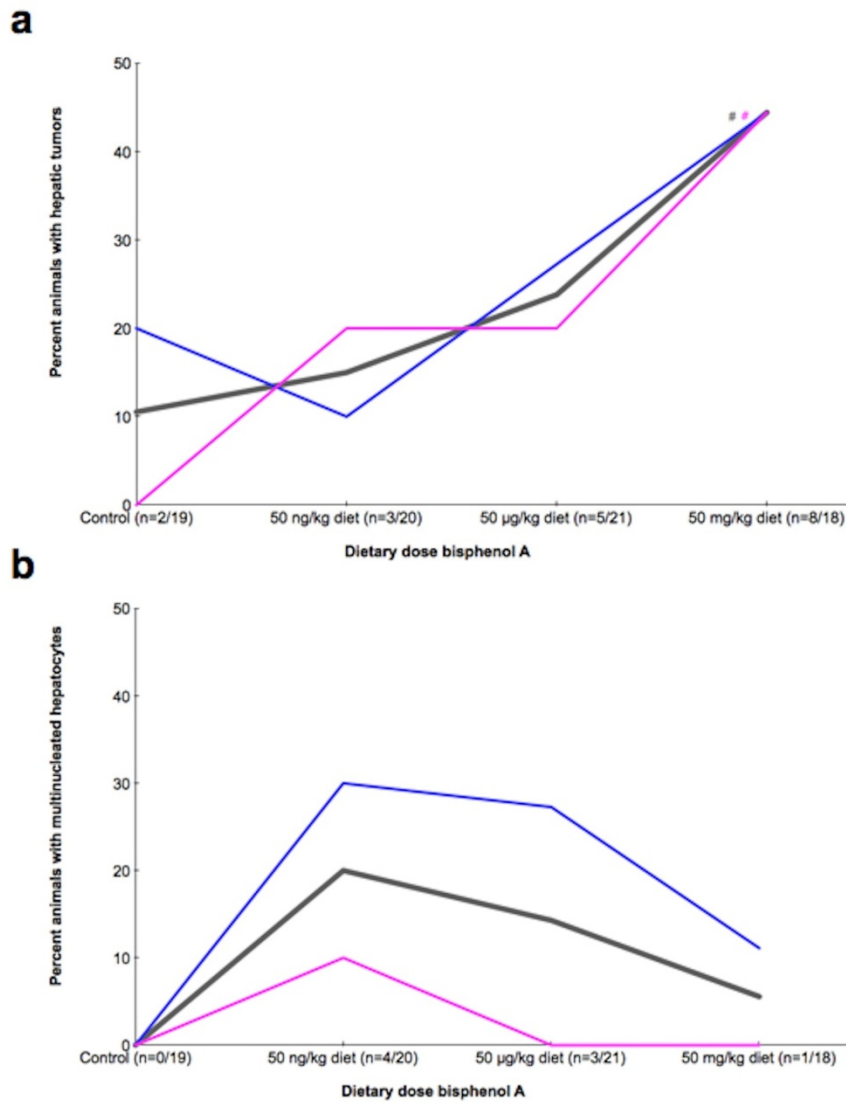
Figure 2.2 Mice exposed perinatally to BPA exhibit both linear and non-monotonic dose responses in a lesion-specific manner. *(A)* Mice exposed perinatally to BPA exhibit a statistically significant trend in a combination of neoplastic and preneoplastic hepatic lesions. *(B)* Mice exposed perinatally to BPA exhibit a non-monotonic trend in multinucleated hepatocytes, although this trend is not statistically significant. Gray line and hash symbol indicate total animals. Blue line, and pink line and hash symbol, indicate male and female animals only, respectively. #*p* for trend <0.05 on Cochrane-Armitage exact test of trend and logistic regression (Supplementary Material, Table S2).
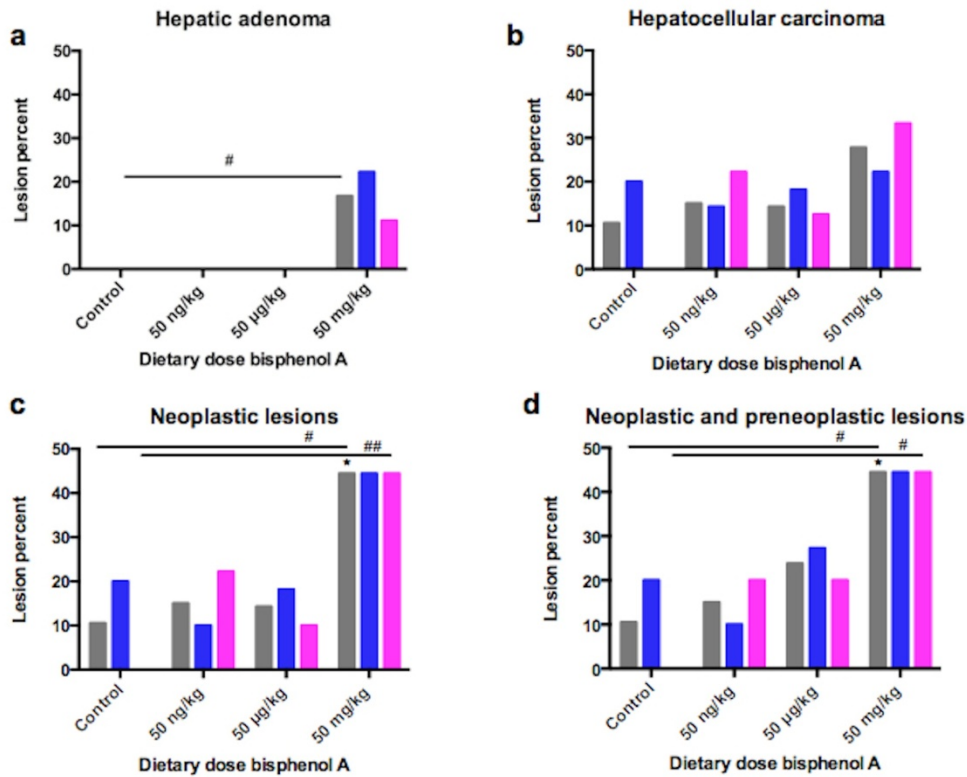
Figure 2.3 Dose-dependent incidence of hepatic tumors in mice exposed perinatally to BPA. *(A)* Mice perinatally exposed to BPA exhibit a statistically significant trend in hepatic adenomas (n=3/78). *(B)* Mice perinatally exposed to BPA exhibit hepatocellular carcinomas (n=13/78). *(C)* Mice perinatally exposed to BPA exhibit a statistically significant trend in neoplastic hepatic lesions (n=16/78). *(D)* Mice perinatally exposed to BPA exhibit a statistically significant trend in neoplastic and preneoplastic hepatic lesions (n=18/78). Gray bars indicate total animals. Blue and pink bars indicate male and female animals only, respectively. Spanning bar in 3A and upper spanning bars in 3C and 3D indicate trends in total animals. Lower spanning bars in 3C and 3D indicate trends in female animals. #*p* for trend <0.05 on both Cochrane-Armitage exact test of trend and logistic regression, with the exception of exact test only for hepatic adenoma. ##*p* for trend <0.1. *Odds ratio *p*<0.05 on logistic regression.
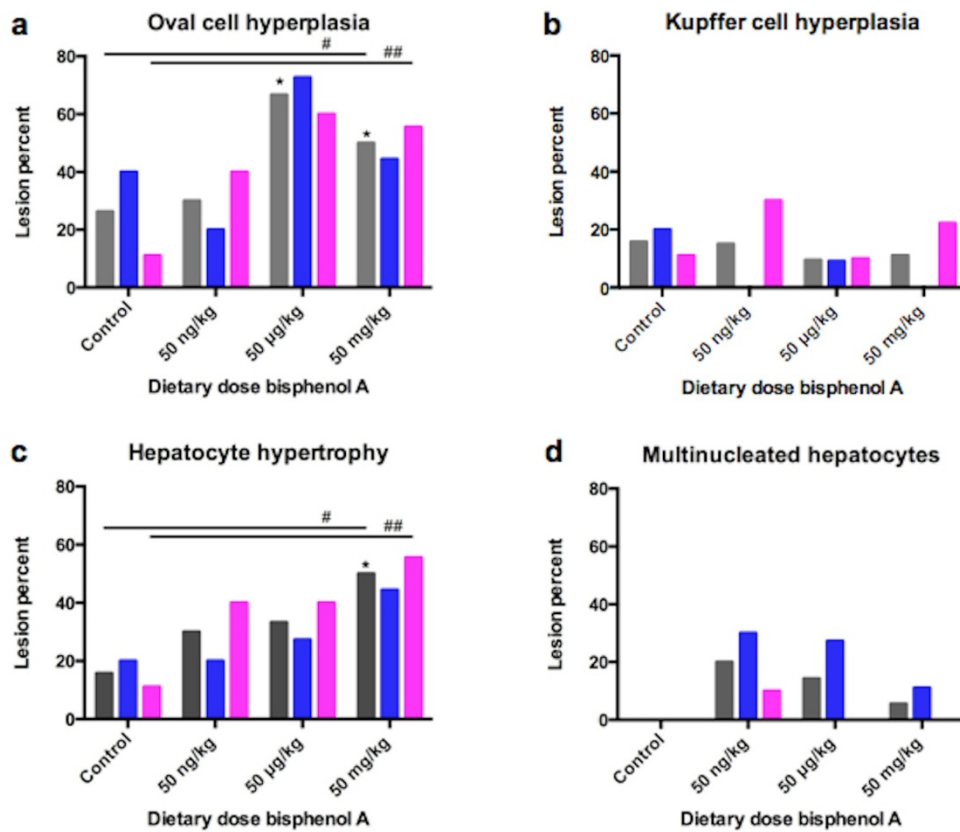
Figure 2.4 Dose-dependent incidence of proliferative lesions in mice exposed perinatally to BPA. *(A)* Mice perinatally exposed to BPA exhibit a statistically significant trend in oval cell hyperplasia. *(B)* Mice perinatally exposed to BPA exhibit no clear trend in Kupffer cell hyperplasia. *(C)* Mice perinatally exposed to BPA exhibit a statistically significant trend in hepatocyte hypertrophy. *(D)* Mice perinatally exposed to BPA exhibit no clear trend in multinucleated hepatocytes. Gray bars indicate total animals. Blue and pink bars indicate male and female animals only, respectively. Upper spanning bars in 4A and 4C indicate total animals. Lower spanning bars in 4A and 4C indicate female animals. #*p* for trend <0.05 on both Cochrane-Armitage exact test of trend and logistic regression.

##*p* for trend <0.1. *Odds ratio *p*<0.05 on logistic regression.

CHAPTER 3

Stat3 is a Candidate Epigenetic Biomarker of Murine Perinatal Bisphenol A Exposure Associated with Murine Hepatic Tumors with Implications for Human Health

3.1   Abstract

Bisphenol A (BPA) is an endocrine disrupting chemical (EDC) that has been implicated as a potential carcinogen and epigenotoxicant. We have previously reported dose-dependent incidence of hepatic tumors in 10-month-old isogenic mice perinatally exposed to BPA through maternal diet (50 ng, 50 µg, or 50 mg BPA/kg diet, or a phytoestrogen-free control diet). In order to investigate potential developmental origins of this observation, we evaluated DNA methylation via bisulfite sequencing at three candidate genes (*Esr1*, *Il-6st*, and *Stat3*) in liver tissue of BPA-exposed mice euthanized at two timepoints: post-natal day 22 (PND22; n=147) or 10-months of age (n=78, including n=18 with hepatic tumors). In addition, DNA methylation profiles were analyzed at human homologs of murine candidate genes in human fetal liver samples (n=50) with known liver tissue BPA levels. Candidate genes were chosen based on reported expression changes in both rodent and human hepatocellular carcinoma. Regions for bisulfite sequencing were chosen by mining whole genome next generation sequencing methylation datasets of both mice and human liver samples with known perinatal BPA exposures. One of three candidate genes that we tested with this method, *Stat3*, displayed dose-dependent DNA methylation changes in 10-month mice with liver tumors as compared to those without liver tumors, as well as dose-dependent methylation changes in 3-week sibling mice

51

from the same exposure study, implicating *Stat3* as a potential epigenetic biomarker of both early life BPA exposure and adult disease in mice. DNA methylation profiles varied with liver tissue BPA level in human fetal liver samples, as well, suggesting *STAT3* may be a translationally relevant candidate biomarker. These data implicate *Stat3* as a potential early life biomarker of adult murine liver tumor risk following early BPA exposure with early evidence of relevance to human health. The characterization of environmentally influenced biomarkers of disease is a crucial next step for the development of novel screening targets for human disease prevention.

3.2   Introduction

Environmental epigenetics, or the study of the impact of environmental exposures on patterns of epigenetic regulation, suggests future public health interventions may reverse deleterious effects of the social, nutritional, and chemical environment to help prevent exposure-linked disease. Environmental exposures that occur during early life development, in particular, have been shown to induce altered epigenetic programs that affect adult health outcomes (Dolinoy et al., 2007; Prins et al., 2008).

We have previously reported a dose-dependent increase in hepatic tumors in 10-month mice that were perinatally exposed to one of three doses of the endocrine disruptor bisphenol A (BPA) (Weinhouse et al., 2014). Notably, a significant increase in liver tumors was evident at 10-months of age, which represents early onset disease in mice. Furthermore, the classical sexual dimorphism of a higher tumor rate in males as compared to females was not present (Weinhouse et al., 2014). Two other studies have implicated BPA as a potential carcinogen in reproductive estrogen-target organs. BPA has been linked to proliferative tissue changes in rat mammary glands (Dhimolea et al., 2014) and to frank prostate cancer in mice with human prostate stem cell xenografts supplemented with sex steroid hormones to mimic human male aging (Prins et al.,

2014a). Additionally, these studies have identified epigenetic alterations linked to BPA dose and tissue alterations, supporting the hypothesis that epigenetic changes may mediate the relationship between early life BPA exposure and adult health outcomes, including cancer (Dhimolea et al., 2014, Prins et al., 2014a).

Epigenetic patterns consist of mitotically heritable marks that govern chromatin organization and gene expression, including DNA methylation, histone tail modifications, and non-coding RNA. These epigenetic changes may serve as evidence of past exposure, risk factors for subsequent disease, and reversible targets of public health or clinical interventions (Bassett and Barnett, 2014; Dolinoy et al., 2007; Shukla and Meeran, 2014). Targeted epigenetic changes, including promoter hypermethylation of tumor suppressors and panels of microRNAs, are currently in use as diagnostic biomarkers in the laboratory and clinic for lung, colorectal, and prostate cancers (Sandoval et al., 2013). In order to facilitate translation of animal studies that identify epigenetic biomarkers of environmental exposure and disease risk to human health and disease prevention, studies must demonstrate epigenetic changes not only at a single time-point but across the life-course, and validate with mechanistic and epidemiological studies. Manikkam *et al.* reported exposure-specific epigenetic signatures using epigenome-wide discovery approaches for detection of epigenetic changes in sperm of mice exposed to endocrine disruptors (2012). However, several studies have demonstrated the presence of stochastic and global epigenomic changes following environmental exposures in mice (Dolinoy et al., 2006; Weinhouse et al., 2011) and humans (Dominguez-Salas et al., 2014), suggesting that targeted, toxicant-specific epigenetic changes may be difficult to identify.

In order to address concerns with past candidate gene epigenetic studies, we employed a novel method for detection of candidate epigenetic biomarkers in this study. We chose

53

translationally relevant candidate genes with functional links to hepatocellular carcinoma for analysis based on expression changes reported in the literature in both rodent and human liver tumors. Three candidate genes were chosen: *estrogen receptor α* (*Esr1/ESR1*) (Dai et al., 2014; Kazantseva, Yarushkin, & Pustylnyak, 2013; Lau, Han, Hu, & Ji, 2013; W.-H. Liu et al., 2009); *interleukin 6 signal transducer (Il6st/IL6ST*) (Bioulac-Sage et al., 2010; Rosell et al., 2009; Shi et al., 2014b; Umemura et al., 2014) which codes for the *IL-6* co-receptor gp130, and *signal transducer and activator of transcription 3* (*Stat3/STAT3*) (Rebouissou et al., 2009; Rosell et al., 2009). Further, these candidate genes are functionally linked. Increased production of the cytokine IL-6 initiates downstream STAT3 signaling (Rosell et al., 2009; Shi et al., 2014a). STAT3 signaling is a key event in inflammation-driven liver carcinogenesis (Rosell et al., 2009). In fact, the classical sexual dimorphism in HCC incidence is thought to be due to the anti-inflammatory influence of endogenous estrogen via suppression of IL-6 production in an ERα-dependent manner (Shi et al., 2014b). BPA has been shown to increase expression of both IL-6 and STAT3 via both ERα and ERβ in human hepatoma Hep3b cells (Sekine et al., 2004). In order to identify short regions for quantitative bisulfite sequencing within these candidate genes, we mined existing whole genome next generation sequencing methylation datasets for windows that exhibited lability in DNA methylation profiles following perinatal BPA exposure in both mice (Kim et al., 2014) and humans [unpublished data] (MethylPlex, Rubicon Genomics, Ann Arbor). This approach allowed us to combine a traditional candidate gene approach, suitable for highly quantitative bisulfite sequencing on the Sequenom EpiTYPER MassARRAY platform, with epigenome-wide assessments of regions of altered methylation associated with early life BPA exposure, to identify candidate biomarkers linked to both exposure and disease.

Here, we provide proof of principle for a novel method for identification of epigenetic biomarkers of exposure and outcome across the life-course and across species. We demonstrate our method's ability to detect epigenetic changes associated with perinatal BPA exposure and liver tumor status in 10-month mice, as well as in 3-week sibling mice from the same exposure study, suggesting that alterations at these loci may serve as candidate early life epigenetic biomarkers for detection of exposure and estimation and potential mitigation of disease risk. Further, we include human fetal liver tissue characterized for BPA levels to demonstrate early translation of candidate biomarkers identified herein. Our approach combines highly quantitative bisulfite sequencing with semi-agnostic data mining of epigenome-wide datasets to detect epigenetic biomarkers of both exposure and outcome in rodents and humans. Studies that combine *in vivo* animal models in controlled experimental environments with *in vitro* mechanistic and human epidemiological cohort validation will be a powerful approach for detection of epigenetic changes with definitive links to exposure and outcome with relevance to human health.

3.3   Materials and Methods

3.3.1   Mouse and Human Liver Samples

Mice were obtained from a colony generated by backcrossing C3H/HeJ mice carrying the viable yellow *Agouti* (A^{vy}) allele with C57BL/6J mice, followed by >200 generations of sibling mating (Waterland & Jirtle, 2003). The A^{vy} strain is isogenic (Waterland & Jirtle, 2003) and has been empirically confirmed to be genetically 93% C57BL/6J (Weinhouse et al., 2014). Offspring of virgin wild-type (*a/a*) females and heterozygous (A^{vy}/a) males were exposed during gestation and lactation to one of three doses of BPA (50 ng, 50 μg, or 50 mg BPA/kg maternal diet) or to a phytoestrogen-free control diet, as previously described (Weinhouse et al., 2014). This mating

scheme produced approximately 50% wild-type (*a/a*) offspring and approximately 50% heterozygous (A^{vy}/*a*) offspring. The majority of A^{vy}/*a* mice were euthanized on post-natal day (PND) 22. A subset of wild-type (*a/a*) mice (approximately 1 male and 1 female per litter for each BPA diet group) were then housed with a same-sex A^{vy}/*a* sibling and fed the standard phytoestrogen-free control diet until they were euthanized at 10 months of age, as described by Anderson et al. (Anderson et al., 2013) (**Table 3.1**). During dissection of both PND22 and 10-month animals, liver tissue was collected and flash frozen in liquid nitrogen. Liver tissue from 10-month animals was evaluated for histopathologic lesions, including benign and malignant tumors, as previously described by Weinhouse et al. (Weinhouse et al., 2014). Grossly visible lesions from tumor-bearing mice were dissected by a board-certified veterinary pathologist (ILB) for analysis in this study. In addition, human fetal liver tissue, gestational day 74-120, was analyzed in this study, to assess potential relevance of mouse results to human liver epigenetics. Human fetal liver tissue was obtained from the University of Washington Laboratory for the Study of Human Embryology (LSHE) fetal tissues bank (2R24 HD000836-47) (Nahar et al., 2013). These clinical liver samples were taken from voluntary 1st and 2nd trimester pregnancy terminations, with appropriate consent from donors (Nahar et al., 2013). These samples meet criteria for IRB exemption for human subject research (UM IRB exemption: HUM00024929). No identifying information other than gestational age, race, and sex were provided to researchers. Liver tissue measurements for free and conjugated (glucuronidated and sulfated) BPA in PND22 mouse liver samples (Anderson et al., 2012b) and human fetal liver samples (Nahar et al., 2013) have confirmed liver BPA levels within the range of reported human environmental exposures (Laura N Vandenberg et al., 2012).

3.3.2 Candidate Gene Assay Design

In order to identify short regions (approximately 400-600bp) for bisulfite sequencing within these candidate genes, we mined whole genome next generation sequencing methylation datasets for 150bp windows that exhibited lability in DNA methylation profiles following perinatal BPA exposure in both mice (Kim et al., 2014) and humans [unpublished data] (MethylPlex, Rubicon Genomics, Ann Arbor). Regions of altered methylation (RAMs; 100bp windows with 50bp overlap) within candidate genes that exhibited differential methylation (p<0.05) in at least two consecutive windows (150bp) in at least two of three comparisons tested (control vs. 50 µg BPA/kg maternal diet, control vs. 50 mg BPA/kg maternal diet, and 50 µg BPA/kg maternal diet vs. 50 mg BPA/kg maternal diet in mouse data; low BPA tertile vs. medium BPA tertile, low BPA tertile vs. high BPA tertile, and medium BPA tertile vs. high BPA tertile in human data) were chosen for bisulfite sequencing (**Table 3.2**).

3.3.3 Bisulfite Sequencing of Candidate Genes

Genomic DNA was isolated from 10-month (n=78; **Table 3.1**) and PND22 (n=147; **Table 3.1**) mouse liver tissue samples and from human fetal liver samples (n=50) using buffer ATL, proteinase K, and RNase A (QIAGEN Inc., Valencia, CA), followed by phenol-chloroform extraction and ethanol precipitation. DNA quality and concentration was assessed using a ND1000 spectrophotometer (NanoDrop Technology, Wilmington, DL). Quantitative DNA methylation patterns at candidate biomarker genes were analyzed via sodium bisulfite treatment followed by sequencing using Sequenom EpiTYPER MassARRAY technology. Sodium bisulfite treatment was performed using the QIAGEN EpiTect Bisulfite Kit (QIAGEN) with approximately 1 µg input genomic DNA. EpiTYPER assays were designed using the Sequenom EpiDesigner tool (www.epidesigner.com), and candidate primer sets were assessed for unique products in the bisulfite-converted mouse and human genomes using the BiSearch ePCR tool

(http://bisearch.enzim.hu). PCR was carried out in 25 µl reactions using approximately 50 ng of bisulfite-converted DNA, HotStarTaq master mix (QIAGEN Inc., Valencia, CA) and forward and reverse (0.1 pmol each) primers under the following conditions: 15 minutes at 95ºC, 40 cycles of (30 seconds at 94ºC, 30 seconds at annealing temperature (T_A), 1 minute at 72ºC), 10 minutes at 72ºC. Primer sequences for bisulfite sequencing are listed in **Table 3.3**.

3.3.4   mRNA Expression Analysis via qPCR

RNA was purified from 10-month mouse liver tissue samples (n=78), a subset of PND22 mouse liver tissue samples (n=38; n=10 control, n=18 50 µg BPA/kg diet; n=10 50 mg BPA/kg diet), and human fetal liver samples (n=50) using RNeasy Mini Kit or All-Prep Kit (QIAGEN). Briefly, approximately 10-15 mg of liver tissue was homogenized using three 30 second bursts at 60 Hz in a TissueLyser II (QIAGEN). Crude lysates were processed on a QIAcube automated nucleic acid purification system using manufacterer's kit instructions. Total RNA quality and concentration for human fetal liver samples was assessed using Agilent BioAnalyzer, as previously described (Nahar et al., 2013). Total RNA quality and concentration for mouse liver samples was assessed using a ND1000 spectrophotometer (NanoDrop Technology.) For each sample, approximately 500ng of total RNA was used with the iScript cDNA Synthesis Kit (Bio-Rad, Hercules, CA) to generate cDNA for downstream real time qPCR (RT-qPCR). Primer sequences for qPCR are listed in **Table 3.4**. Reference genes were empirically confirmed to be invariant across treatment groups during data analysis. All RT-qPCR primers were verified for product uniqueness using Primer BLAST (www.ncbi.nlm.hih.gov/tools/primer-blast/). Most primers span introns or exon-exon junctions to avoid amplification of genomic DNA. All primer sets were tested for PCR efficiency using 10-fold serial dilutions of a standard template and plotting of standard curves. Amplification of cDNA was carried out in 25ul reactions using iQ

SYBR Green Supermix (Bio-Rad, Hercules, CA). Each reaction contained 1 μl of cDNA template and 100 nM primer concentration. All experimental and reference reactions were run in duplicate on a C100 Thermal Cycler with a CFX96 Real-Time head (Bio-Rad). Each plate contained no template controls for each primer set, as well as two reference genes per species per assay (*Gapdh* and *B2m* for mouse samples, *GAPDH* and *UBC* for human samples). The average threshold cycle (*C(t)*) from duplicate reactions was calculated for individual genes using CFX Manager Version1.6 software (Bio-Rad.) Expression values were normalized to endogenous reference genes by first averaging *C(t)* values for both reference genes for each sample and then subtracting the average reference value from the experimental *C(t)* value.

3.3.5   Data Analysis

3.3.5.1 Analysis of Bisulfite Sequencing Data in Mouse Liver Samples

Hypothesized dose-dependent DNA methylation changes in 10-month mice with tumors, as compared to 10-month mice without tumors, as well as dose-dependent DNA methylation changes at the same epigenetic loci in sibling 3-week mice from the same exposure study were assessed using repeated measures mixed models (PROC MIXED), with individual CpG sites defined as repeated measures and litter as the random intercept, in order to account for lack of independence of multiple CpG sites at a single locus within an individual animal. Fixed effects of the dependent variable assessed associations between dose and tumor status with average methylation at a locus. Dose variables were assessed on a natural scale, rather than an ordinal scale, to more closely model the true exposure and to facilitate practical interpretation of results. As natural scale dose variable coding has increased power to detect dose-based differences as compared to ordinal scale dose variable coding, results were confirmed with additional models

run with ordinal scale dose variables, to facilitate easy comparison with a prior study using an ordinal scale dose variable for statistical analyses (Weinhouse et al., 2014).

We tested for the presence of dose-dependent DNA methylation changes by tumor status in 10-month mouse liver samples (n=78; **Table 3.1**), both with and without liver tumors, using a total of 12 models, including four models per candidate gene (dependent variable as average DNA methylation): Model 1 contained four predictors, including a repeated measure variable for percent methylation at each CpG site, a dose predictor, a dichotomous tumor status variable, and an interaction variable (*dose*tumor*), to test for dose-dependent differences in average DNA methylation by tumor status (**Figures 3.1B, 3.6B, 3.11B**); Model 2 included repeated CpG site predictor and dose predictor, and adjusted for both sex and tumor status to assess dose-dependent changes in average DNA methylation independent of tumor status (**Figure 3.2B, 3.7B, 3.12B**); Model 3 included the previous predictors but contained an alternate interaction variable (*dose*CpG site*) to assess site-specific differences in DNA methylation; and the fourth model tested for a monotonic trend in DNA methylation with dose.

To investigate dose-dependent DNA methylation patterns in sibling PND22 mice from the same exposure study (n=147; **Table 3.1**), we ran a total of nine final models on PND22 mouse liver samples, including three models per candidate gene (dependent variable as average DNA methylation):   (**Figures 3.3A, 3.8A, 3.13A**); the second model containing the previous two predictors and an additional interaction variable (*dose*CpG site*) to assess site-specific DNA methylation changes with dose (**Figures 3.3B, 3.8B, 3.13B**); and the third model testing for monotonic trend in DNA methylation change with dose. Mixed models for PND22 mouse liver samples were adjusted for sex and genotype and included a random intercept to cluster data by litter. Genotype was included in the final models as a potential confounder after confirmation

that an interaction variable (*dose*genotype*) was not significant at any candidate gene, indicating that DNA methylation did not vary across genotypes with exposure.

3.3.5.2 Analysis of Bisulfite Sequencing Data in Human Fetal Liver Samples

Hypothesized dose-dependent DNA methylation changes in human fetal liver samples at human homologs of murine candidate genes were assessed using the four repeated measures mixed models described above, with individual CpG sites defined as repeated measures, in order to account for lack of independence of multiple CpG sites at a single locus within an individual. Similarly, fixed effects of the dependent variable assessed associations between dose and tumor status with average methylation at a locus. BPA exposure was coded both as a categorical variable (binned into tertiles) and a continuous variable, for both free and total BPA measurements. Free and conjugated BPA liver tissue measurements were performed in these samples by Nahar, et al (2013), as previously described. A total of four models were run for candidate genes *ESR1* and *IL-6ST* (dependent variable average methylation). The first two models contained four predictors, including a repeated measure variable for percent methylation at each CpG site, and categorical dose predictor, one model each for total and free BPA measurements, as well as a dichotomous sex variable and continuous gestational age variable, to adjust for potential confounding (**Figures 3.4**, **3.5**, **3.9**, and **3.10**). The second two models contained the same four predictors, albeit with continuous dose predictors, one model each for total and free BPA measurements. A total of six models were run on candidate gene *STAT3*. As continuous free and total BPA were significantly associated with average methylation at *STAT3* (**Figures 3.14** and **3.15**), two additional models were run containing quadratic dose terms (*(centered free BPA)^2* and *(centered total BPA)^2*, respectively) (**Figures 3.16** and **3.17**) to assess

61

the presence of a parabolic, non-monotonic dose-response curve visually apparent at CpG site 1 with categorical BPA predictors (**Figures 3.14** and **3.15**).

3.3.5.3 Analysis of mRNA Expression Data

The average threshold cycle (*C(t)*) from duplicate reactions was calculated for individual genes using CFX Manager Version1.6 software (Bio-Rad). Expression values were normalized to endogenous reference genes to obtain *ΔC(t)* values by first averaging *C(t)* values for both reference genes for each sample and then subtracting the average reference value from the experimental *C(t)* value. Expression values for *Stat3* or *STAT3* were then assessed for association with perinatal BPA exposure (*ΔΔC(t)*) via simple linear regression models (PROC REG). Regression models for mouse samples were run separately for 10-month and PND22 mice, and were adjusted for sex and tumor status in the first and for sex and genotype in the second. Dose-dependent differences in expression of *Stat3* in 10-month animals by tumor status were assessed by including an interaction variable (dose*tumor status) in subsequent models. Regression models for human samples were adjusted for sex and gestational age. BPA exposure was coded both as a categorical variable (binned into tertiles) and a continuous variable, for both free and total BPA measurements. Each endogenous reference gene was analyzed in separate linear regression models, to empirically confirm references to be invariant by BPA exposure. Regression coefficients (β coefficients) were used to calculate fold-change values [$100(e^\beta-1)$], with p-values <0.05 reported as statistically significant differences. All statistical analyses were performed in SAS v9.2 (SAS, Cary, NC).

3.4.   Results

3.4.1. Candidate Gene DNA Methylation in Mice and Humans

3.4.1.1.   *Esr1/ESR1*

3.4.1.1.1. *Esr1* Methylation in 10-month Mouse Livers

Average percent DNA methylation at two CpG sites within murine *Esr1* (**Table 3.5**) in 10-month mice did not differ by tumor status in any dose group. No differences by sex were noted (p=0.58). Analyses of BPA dose alone, controlling for tumor status, did not reveal any statistically significant differences in average or site-specific DNA methylation (**Table 3.6**).

3.4.1.1.2 *Esr1* Methylation in Sibling PND22 Mouse Livers

DNA methylation at the same two CpG sites within murine *Esr1* (**Table 3.2**) was analyzed in sibling PND22 mice from the same exposure study for evidence of early life perturbation of epigenetic patterning. After adjustment for sex and genotype, no differences in average or site-specific DNA methylation were seen at *Esr1* in PND22 mice (**Table 3.7**).

Similar to 10-month mice, no sex differences in *Esr1* DNA methylation were noted in PND22 mice (p=0.40). In addition, no differences were noted between animals based on genotype at the *agouti* locus (p=0.26).

3.4.1.1.3 *ESR1* Methylation in Human Fetal Livers

Neither average nor site-specific DNA methylation at two CpG sites in the human homolog *ESR1* (**Table 3.2**) in human fetal liver samples differed by tertile of total (combined free and conjugated) liver tissue BPA (**Table 3.8**). The lack of association between average percent DNA methylation and binned total BPA was also evident when total BPA was modelled as a continuous variable (p=0.71).

When the analysis was restricted to free BPA only, the medium tertile exhibited an approximate 4.5% decrease in average methylation as compared to the lowest (p=0.04) tertile (medium BPA: 55.4%, 95% CI: 53.9-56.9%; low BPA: 59.9%, 95% CI: 58.2-61.7%) (**Table**

3.9). No differences in DNA methylation were seen at CpG site 1 (**Table 3.9**). No association was noted between average percent DNA methylation and continuous free BPA (p=0.67).

No differences in average percent DNA methylation were noted between sexes in models adjusting for total BPA (p=0.67) or free BPA (p=0.57). No associations between average percent DNA methylation and continuous gestational age were seen when adjusting for total BPA (p=0.94) or free BPA (p=0.83).

3.4.1.2.   *Il-6st/IL-6ST*

3.4.1.2.1. *Il-6st* Methylation in 10-month Mouse Livers

Average percent DNA methylation at three CpG sites within murine *Il-6st* in 10-month mice with tumors was ~3% lower in the 50 mg group as compared to animals without tumors (p=0.03) (**Table 3.10**). Analyses of BPA dose alone, controlling for tumor status, did not reveal any statistically significant differences in average or site-specific DNA methylation (**Table 3.11**). No differences by sex were noted (p=0.06).

3.4.1.2.2. *Il-6st* Methylation in Sibling PND22 Mouse Livers

Average and site-specific percent DNA methylation at the same three CpG sites within murine *Il-6st* (**Table 3.12**) were analyzed in sibling PND22 mice for evidence of early epigenetic changes with the potential to persist into adulthood. Following adjustment for sex and genotype, no significant differences in average methylation were seen in any dose group (**Table 3.12**). When methylation patterns were analyzed by individual CpG site, differences at CpG site 1 and CpG site 3 not seen in 10-month mice were evident in 3-week sibling mice. Approximately 9% hypermethylation at CpG site 1 was seen in the 50 μg group, as compared to control (50 μg: 81.1%, 95% CI: 77.7-84.4%; control: 71.9%, 95% CI: 69.0-74.8%; p=0.04) (**Table 3.12**). CpG site 3 was approximately 5% hypomethylated as compared to control in the 50 ng group (50 ng:

64

79.3%, 95% CI: 77.5-81.1%; control: 84.0%, 95% CI: 81.5-86.5%) p=0.04) (**Table 3.12**). No differences were seen at CpG site 2 in any dose group (**Table 3.12**). DNA methylation did not differ by sex (p=0.09) or genotype (p=0.05).

3.4.1.2.3 *IL-6ST* Methylation in Human Fetal Livers

Average DNA methylation across seven CpG sites in the human homolog *IL-6ST* (**Table 3.2**) in human fetal liver samples did not differ by tertile of total (combined free and conjugated) liver tissue BPA (**Table 3.13**). When percent methylation was analyzed at individual CpG sites, approximately 4% hypomethylation at CpG site 5 was seen in the high tertile as compared to the medium tertile of total BPA (high BPA: 89.2%, 95% CI: 88.1-90.3%, medium BPA: 93.3%, 95% CI: 92.1-94.5%; p=0.02) (**Table 3.13**). The high tertile of total BPA was also~5-6% hypomethylated at CpG site 7 as compared to the medium tertile (p=0.01) and the low tertile (p<0.01) (high BPA: 81.7%, 95% CI: 80.3-83.0%, medium BPA: 87.0%, 95% CI: 85.5-88.4%, low BPA: 88.0%, 95% CI: 86.6-89.3%) (**Table 3.13**). No association between average percent DNA methylation and binned total BPA was evident when total BPA was modelled as a continuous variable (p=0.33).

When the analysis was restricted to free BPA only, no statistically significant difference in average DNA methylation were seen between any two tertiles (**Table 3.14**). Similar to total BPA analyses, CpG site 7 was approximately 3-5% hypomethylated in the high tertile of free BPA as compared to the medium (p=0.02) and low tertiles (p=0.01) (high BPA: 82.6%, 95% CI: 81.1-84.0, medium BPA: 86.0%, 95% CI: 84.5-87.5%, low BPA: 88.0%, 95% CI: 86.6-89.4% (**Table 3.14**). No association was noted between average percent DNA methylation and continuous free BPA (p=0.59).

No differences in average percent DNA methylation were noted between sexes in models adjusting for total BPA (p=0.17) or free BPA (p=0.15). No associations between average percent DNA methylation and continuous gestational age were seen when adjusting for total BPA (p=0.52) or free BPA (p=0.51).

3.4.1.3 *Stat3/STAT3*

3.4.1.3.1 *Stat3* Methylation in 10-month Mouse Livers

Average percent DNA methylation at three CpG sites within murine *Stat3* (**Table 3.2**) in 10-month mice with tumors was ~7% lower in the 50 µg group (p=0.01) as compared to animals without tumors (**Table 3.15**, **Figure 3.1**).

Site-specific analysis showed that CpG site 2 was ~4% hypermethylated in the 50 mg group, as compared to control (p=0.04) (**Table 3.16**, **Figure 3.2**). No differences were observed in DNA methylation by sex (p=0.06).

3.4.1.3.2 *Stat3* Methylation in Sibling PND22 Mouse Livers

Average percent DNA methylation at the same three CpG sites within murine *Stat3* (**Table 3.2**, **Figure 3.3**) was analyzed in sibling PND22 mice for evidence of early epigenetic changes with the potential to persist into adulthood. Following adjustment for sex and genotype, an approximately 2-3% decrease in average methylation were seen in the two highest dose group (50 µg BPA/kg maternal diet: 83.5%, 95% CI: 82.7-84.3%, p<0.01; 50 mg BPA/kg maternal diet: 84.7%; 95% CI: 84.1-85.2%; p=0.01) as compared to control (86.7%; 95% CI: 86.1-87.3%) (**Table 3.17**, **Figure 3.3**). When methylation patterns were analyzed by individual CpG site, hypomethylation was noted at all three CpG sites sequenced. Approximately 2.5% hypomethylation at CpG site 1 was seen in the 50 µg group, as compared to control (50 µg: 85.3%, 95% CI: 84.4-86.3%; control: 87.9%, 95% CI: 87.2-88.6%; p=0.03) (**Table 3.17**, **Figure**

3.3). Approximately 2-3% hypomethylation was seen in the lowest and highest dose groups at CpG site 2 (50 ng: 85.4%, 95% CI: 84.8-86.0%, p=0.01; 50 mg: 83.3%, 95% CI: 82.7-84.0%, p<0.01) as compared to control (86.8%, 95% CI: 86.0-87.5%) (**Table 3.17**, **Figure 3.3**). Similar differences (~1-5% hypomethylation) were seen at CpG site 3 in all dose groups (50 ng: 84.8%, 95% CI: 84.2-85.5%, p<0.01; 50 µg: 80.7%, 95% CI: 79.7-81.7%, p=0.01; 50 mg: 83.9%, 95% CI: 83.1-84.6%, p<0.01; control: 85.5%, 95% CI: 84.7-86.3%) (**Table 3.17**, **Figure 3.3**).

A small but statistically significant increase (~1%) in average DNA methylation was noted in males as compared to females at *Stat3* in PND22 mice (males: 85.9%, 95% CI: 85.5-86.3%; females: 84.5%, 95% CI: 84.0-85.0%; p=0.01). This effect was not seen in bivariate models between sex and average methylation or in models containing interaction variables (*sex*dose*), indicating that no strong sex-based differences in methylation were present. No difference in average methylation was noted between animals based on genotype at the *agouti* locus (p=0.47).

3.4.1.3.3 *STAT3* Methylation in Human Fetal Livers

Neither average nor site-specific DNA methylation at three CpG sites in the human homolog of *STAT3* (**Table 3.2**) in human fetal liver samples differed by tertile of total (combined free and conjugated) liver tissue BPA (**Table 3.18**, **Figure 3.4**) or free BPA alone (**Table 3.19**, **Figure 3.5**). However, statistically significant associations with average percent DNA methylation were evident when total BPA (p=0.01) and free BPA (p=0.02) were modelled as continuous variables (**Tables 3.18** and **3.19**, **Figures 3.6** and **3.7**). Mean-centered squared variables (*(centered total BPA)^2* and *(centered total BPA)^2*) were statistically significant when added to the models (p=0.01 and p=0.04, respectively), confirming a non-monotonic dose-response visually apparent at CpG site 1 (**Figures 3.6 and 3.7**).

No differences in average percent DNA methylation were noted between sexes in models adjusting for total BPA (p=0.22) or free BPA (p=0.23). No associations between average percent DNA methylation and continuous gestational age were seen when adjusting for total BPA (p=0.34) or free BPA (p=0.28).

3.4.2 Candidate Gene Expression

As altered DNA methylation was noted at *Stat3* in mice and *STAT3* in human tissues, we analyzed transcript levels of both genes to investigate a possible functional outcome linked to the observed epigenetic change.

Stat3 expression did not differ by perinatal BPA dose group in 10-month mice (**Figure 3.8**). Tumor status was not linked to *Stat3* mRNA transcript level across dose groups (p=0.79) or in a dose-dependent manner (*dose*tumor* p=0.83) (**Figure 3.8**). Endogenous reference genes did not differ by perinatal dose group (*B2m* p=0.63, *Gapdh* p=0.97; adjusted for sex) or tumor status (*B2m* p=0.14, *Gapdh* p=0.77), confirming their appropriate use as internal controls invariant to experimental exposure and outcome. A decrease in *Stat3* expression with increasing perinatal BPA exposure approached significance in PND22 mice (fold-change for 50 ng group 0.40, 50 μg group 0.23, 50 mg group 0.33; p=0.05; adjusted for sex) (**Figure 3.9**). Endogenous reference genes did not differ by perinatal dose group (*B2M* p=0.80, *Gapdh* p=0.80; adjusted for sex), confirming their appropriate use as internal controls.

Human fetal livers exhibited no change in *STAT3* expression with continuous total (p=0.52) or free BPA (p=0.45), following adjustment for sex and gestational age (**Figures 3.10 and 3.11**). Gestational age was significant in fully adjusted models (total BPA p<0.01, free BPA p<0.01), but interaction variables indicated that the link between age and *STAT3* expression was not dose-dependent (total BPA*gestational age p=0.91, free BPA*gestational age p=0.75).

Human endogenous references genes did not differ by continuous total BPA (GAPDH p=0.60, UBC p=0.52) or free BPA (GAPDH p=0.38, UBC p=0.16), even following adjustment for sex and gestational age, indicating chosen internal controls were invariant with exposure.

3.5   Discussion

Here we show proof of principle for a novel method for detection of candidate epigenetic biomarkers associated with both early life exposure and adult disease across the lifespan and across species. We focused this modified candidate gene study on *Esr1*, *Il-6st*, and *Stat3*, three candidate genes with reported expression differences in both rodent and human HCC. We investigated DNA methylation patterns within regions of these three genes that were empirically demonstrated to be labile following perinatal exposure to BPA in three sample groups: 10-month mice with and without liver tumors perinatally exposed to BPA, sibling PND22 mice from the same exposure study, and human fetal livers with known tissue BPA levels. Tumor status was not associated with DNA methylation at *Esr1* in 10-month mice, but BPA exposure was associated with hypermethylation at this locus in sibling PND22 mice and hypomethylation in human fetal livers, indicating that *Esr1* methylation may be altered by BPA exposure but is not linked to the liver tumor phenotype described in Chapter 2. DNA methylation at human homolog *ESR1* decreased with low level BPA exposure and increased with higher exposure, supporting a potentially non-linear epigenetic response to BPA. These results support *Esr1* as a potential target of BPA-induced DNA methylation change, but do not implicate this candidate gene as a candidate biomarker of both exposure and disease in this study. *Esr1* may exert its effects via DNA methylation changes outside of the region assayed or through other epigenetic or non-epigenetic changes not measured here. Alternatively, *Esr1* may not be involved in the mechanism linking perinatal BPA exposure to liver tumors in these mice.

DNA methylation at the second candidate gene, *Il-6st*, was both increased in 50 mg-exposed mice with tumors and decreased in 50 ng-exposed mice with tumors, as compared to mice without tumors, supporting an interaction between dose and tumor status. Sibling PND22 mice showed decreased methylation at the 50 ng dose and increased methylation at the 50 μg dose at *Il-6st*, a nearly opposite pattern from the one seen in 10-month animals with tumors, suggesting that exposure and outcome may have antagonistic effects on DNA methylation patterns. DNA methylation at the human homolog *IL-6ST* demonstrated hypomethylation with BPA exposure at specific CpG sites, but analysis of total and free BPA as continuous variables indicated no association between BPA exposure and average methylation at this locus. These data implicate Il-6st as a candidate epigenetic biomarker of exposure and disease in mice that may not be relevant to human BPA exposure.

The third candidate gene that we tested with this method, *Stat3,* displayed hypomethylation with tumor status and hypermethylation with increasing BPA exposure in 10-month mice, as well hypermethylation with increasing BPA exposure in 3-week sibling mice from the same exposure study, implicating *Stat3* as a potential epigenetic biomarker of both early life BPA exposure and adult disease in mice. DNA methylation displayed non-monotonic dose-responses to continuous total and free liver tissue BPA level in human fetal liver samples, as well, suggesting *STAT3* may be a translationally relevant candidate biomarker and supporting a growing body of literature on low dose effects of endocrine disruptors (Vandenberg et al., 2013).

We note that all three candidate genes chosen for analysis, *Esr1/ESR1*, *Il-6st/IL-6ST*, and *Stat3/STAT3*, exhibited lability in DNA methylation with BPA exposure, indicating our data mining approach is a successful strategy for distinguishing exposure-related epigenetic changes from those associated exclusively with disease status. However, BPA exposure was associated

with both hypomethylation and hypermethylation, with no clear pattern with age or tumor status across candidate loci, supporting the need for validation of candidate epigenetic biomarkers to distinguish spurious findings from true biological markers and to elucidate the mechanisms surrounding the latter.

The presence of a liver tumor at 10-months in mice was associated with hypomethylation at *Il-6st;* in contrast, after controlling for tumor status, perinatal BPA exposure was associated with hypermethylation at the same locus in the same animals, suggesting that dose-related changes may be masked in later life disease states, although disease-related changes may represent a consequence of cancer and may not be important in driving disease development. Previously, we have shown that global DNA methylation levels were approximately 7-9% higher in tail tissue of the same BPA-exposed, 22-day-old mice analyzed in the current study (Anderson et al., 2012), supporting the hypermethylation response to exposure we observed in the current study. In several comparisons, we note differential effects at specific CpG sites, highlighting the possibility for masking of true site-specific effects in studies analyzing average methylation levels only. However, the direction of site-specific effects was not consistent across age groups at the same locus, indicating that DNA methylation profiles may shift with age, and highlighting the need for functional validation of consistent and easily interpretable candidate biomarkers.

Our approach used agnostic epigenome-wide data mining to identify regions of variable DNA methylation of no predetermined genetic context. Four of six candidate gene region assays were located either within introns or at an exon-intron border (**Table 3.2**). Studies that focus exclusively on DNA methylation of CpG islands within 5' gene promoters disregard the potential biological roles of intergenic and intragenic epigenetic patterning, and also the fact that transcription commonly initiates within or between genes (Carninci et al., 2005; Carninci et al.,

2006; Maunakea et al., 2010). Intronic methylation has been shown to have functional relevance to human disease outcomes; differential methylation of gene variants within the second intron of *KCNQ1* affects CTCF binding and confers risk for Beckwith-Wiedemann syndrome (Demars et al., 2014). Functional relevance of intronic methylation patterns in mice has been shown, as well. Intronic enhancer activity in the murine *sf-1/ad4bp* gene is correlated with both DNA methylation pattern and tissue-specific gene expression (Hoivik et al., 2011). Rademacher and colleagues reported that the human genome contains at least 2,000 intronic CpG islands that are not present in the mouse genome, a subset of which show sequence similarities elsewhere in the human genome, suggesting that they arose via retrotransposition (2014). Transposable elements, such as the murine A^{vy} metastable epiallele, have been previously implicated as targets for early environmental effects on the epigenome (Waterland and Jirtle, 2003). These data suggest that the human genome may contain a larger number of intronic epigenetic targets for environmental perturbation than rodents, indicating the importance of including intronic targets in studies evaluating the impact of environmental epigenetics on human health.

Methylation differences reported in this study are small as compared to those reported at the A^{vy} locus in BPA-exposed animals (Dolinoy et al., 2007) and in human liver cancer pathology (Raggi and Invernizzi, 2013), but are similar to effect sizes reported at other epigenetic loci in A^{vy} mice exposed to BPA (Anderson et al., 2012; Kim et al., 2014). Further, several comparisons yielded p-values between 0.05 and 0.1, indicating that several additional data points may have reached our chosen threshold for statistical significant (p<0.05) given a larger sample size and therefore greater power to detect small effect sizes. However, it is similarly possible that repetition of this study in larger sample size would reveal a clear lack of statistical relationships.

Expression differences were not observed at *Stat3* or *STAT3* in this study, but a 1% change in DNA methylation at the *IGF2* DMR in humans exposed to environmental tobacco smoke has been previously linked to an approximate two-fold increase in *IGF2* transcription, indicating the potential functional relevance of small changes in DNA methylation (Murphy et al., 2012). Although combined expression levels of all *Stat3* or *STAT3* variants did not vary with murine BPA exposure in 10-month or PND22 mice, or with measured human liver tissue level in human fetal liver samples, respectively, these results do not definitively rule out the possibility of gene expression changes that may have occurred at a time point not measured here. Since relevant time points of interest in this study range from conception to 10 months of age in mice, we reasonably might expect that successful detection of elusive expression changes would be unlikely, with the possible exception of particularly persistent changes in expression. Several studies suggest consideration of a broader range of potential functional outcomes of altered intronic methylation profiles. Tissue-specific intragenic methylation has been reported alternately to reduce or enhance transcriptional elongation efficiency (Ball et al., 2009; Brenet et al., 2011; Cokus et al., 2008; Flanagan & Wild, 2007; Rauch et al., 2009), which may affect ordering of subsequent cell signaling cascade activation. Intronic methylation may regulate relative expression of gene isoforms, rather than overall gene expression changes. Maunakea et al. utilized large-scale mapping of DNA methylation profiles in the human brain to demonstrate that tissue- and cell type-specific intragenic methylation can regulate alternative gene promoter activity and subsequent differential expression of alternative transcripts within a single cell type (2010). Gelfman and colleagues discovered that exon recognition relies on DNA methylation during co-transcriptional splicing and that alternative exons may be distinguished from constitutive exons by the presence of fewer methylated CpG sites (2013).

The present study represents a high resolution, semi-agnostic method for identifying candidate epigenetic biomarkers, in contrast to wholly agnostic but lower resolution epigenome-wide approach. Our results highlight the need for life-course studies that follow model organisms or humans over one or more relevant life periods in order to identify early epigenetic changes that persist into adulthood. However, our method is intended as a hypothesis-generating tool for selection of candidate biomarkers for further validation. In order to validate *STAT3* as a biomarker of early life BPA exposure and possible early life risk indicator of increased susceptibility to one or more forms of liver tumors or other liver disease in adulthood, this candidate gene would need to be tested in larger epidemiological cohorts to determine its relevance to human health and possible use as a public health screening tool. Animal studies may inform human health risk if the model is well chosen. C57BL/6J mice are epigenetically stable relative to C3H/HeJ and B6C3F1 strains; the latter are commonly used as sensitive models carcinogenesis bioassays (Phillips et al., 2009). The mouse model used in this study is primarily C57BL/6J (Weinhouse et al., 2014) and therefore represents an epigenetically robust model for candidate biomarker detection.

The field of environmental epigenetics is currently in a period of discovery, analogous to the initial period of discovery in genetic linkage and association studies following the initial sequencing of the human genome. Genome-wide association studies and larger scale epidemiologic studies followed early individual-SNP candidate gene studies, increasing our understanding of epistatic effects and spurious results commonly reported in single gene analyses. The novel method described here represents a highly quantitative candidate gene approach that incorporates semi-agnostic data mining in order to direct discovery to labile regions identified via epigenome-wide analysis.

3.6   Conclusion

Here we demonstrate the utility of a novel method for detection of candidate epigenetic biomarkers which combines traditional candidate gene analyses, by selecting genes with known functional links to the health outcome of interest from those reported in the literature, with data mining of whole genome DNA methylation next generation sequencing datasets for short regions within candidate genes that have been empirically confirmed as labile following perinatal BPA exposure. This focused, hypothesis-generating approach highlights the need for life-course studies that follow organisms over one or more relevant life periods in order to identify early epigenetic changes that persist into adulthood. Candidate epigenetic biomarkers require validation via mechanistic studies to determine potential biological role(s) and epidemiological cohort studies to assess public health relevance.

3.7   References

Anderson, O. S., Nahar, M. S., Faulk, C., Jones, T. R., Liao, C., Kannan, K., … Dolinoy, D. C. (2012a). Epigenetic responses following maternal dietary exposure to physiologically relevant levels of bisphenol A. *Environmental and Molecular Mutagenesis*.

Anderson, O. S., Nahar, M. S., Faulk, C., Jones, T. R., Liao, C., Kannan, K., … Dolinoy, D. C. (2012b). Epigenetic responses following maternal dietary exposure to physiologically relevant levels of bisphenol A. *Environmental and Molecular Mutagenesis*.

Anderson, O. S., Peterson, K. E., Sanchez, B. N., Zhang, Z., Mancuso, P., & Dolinoy, D. C. (2013). Perinatal bisphenol A exposure promotes hyperactivity, lean body composition, and hormonal responses across the murine life course. *FASEB Journal : Official Publication of the Federation of American Societies for Experimental Biology*.

Ball, M. P., Li, J. B., Gao, Y., Lee, J.-H., LeProust, E. M., Park, I.-H., … Church, G. M. (2009). Targeted and genome-scale strategies reveal gene-body methylation signatures in human cells. *Nature Biotechnology*, *27*(4), 361–8.

Bassett, S. A., & Barnett, M. P. G. (2014). The Role of Dietary Histone Deacetylases (HDACs) Inhibitors in Health and Disease. *Nutrients*, *6*(10), 4273–4301.

Bioulac-Sage, P., Balabaud, C., & Zucman-Rossi, J. (2010). Subtype classification of hepatocellular adenoma. *Digestive Surgery*, *27*(1), 39–45.

Brenet, F., Moh, M., Funk, P., Feierstein, E., Viale, A. J., Socci, N. D., & Scandura, J. M. (2011). DNA methylation of the first exon is tightly linked to transcriptional silencing. *PloS One*, *6*(1), e14524.

Carninci, P., Kasukawa, T., Katayama, S., Gough, J., Frith, M. C., Maeda, N., … Hayashizaki, Y. (2005). The transcriptional landscape of the mammalian genome. *Science (New York, N.Y.)*, *309*(5740), 1559–63.

Carninci, P., Sandelin, A., Lenhard, B., Katayama, S., Shimokawa, K., Ponjavic, J., … Hayashizaki, Y. (2006). Genome-wide analysis of mammalian promoter architecture and evolution. *Nature Genetics*, *38*(6), 626–35.

Cokus, S. J., Feng, S., Zhang, X., Chen, Z., Merriman, B., Haudenschild, C. D., … Jacobsen, S. E. (2008). Shotgun bisulphite sequencing of the Arabidopsis genome reveals DNA methylation patterning. *Nature*, *452*(7184), 215–9.

Dai, B., Geng, L., Yu, Y., Sui, C., Xie, F., Shen, W., … Yang, J. (2014). Methylation patterns of estrogen receptor α promoter correlate with estrogen receptor α expression and clinicopathological factors in hepatocellular carcinoma. *Experimental Biology and Medicine (Maywood, N.J.)*, *239*(7), 883–890.

Demars, J., Shmela, M. E., Khan, A. W., Lee, K. S., Azzi, S., Dehais, P., … Gicquel, C. (2014). Genetic variants within the second intron of the KCNQ1 gene affect CTCF binding and confer a risk of Beckwith-Wiedemann syndrome upon maternal transmission. *Journal of Medical Genetics*, *51*(8), 502–11.

Dhimolea, E., Wadia, P. R., Murray, T. J., Settles, M. L., Treitman, J. D., Sonnenschein, C., … Soto, A. M. (2014). Prenatal exposure to BPA alters the epigenome of the rat mammary gland and increases the propensity to neoplastic development. *PloS One*, *9*(7), e99800.

Dolinoy, D. C., Huang, D., & Jirtle, R. L. (2007). Maternal nutrient supplementation counteracts bisphenol A-induced DNA hypomethylation in early development. *Proceedings of the National Academy of Sciences of the United States of America*, *104*(32), 13056–61.

Dolinoy, D. C., Weidman, J. R., Waterland, R. A., & Jirtle, R. L. (2006). Maternal genistein alters coat color and protects Avy mouse offspring from obesity by modifying the fetal epigenome. *Environmental Health Perspectives*, *114*(4), 567–72.

Dominguez-Salas, P., Moore, S. E., Baker, M. S., Bergen, A. W., Cox, S. E., Dyer, R. A., … Hennig, B. J. (2014). Maternal nutrition at conception modulates DNA methylation of human metastable epialleles. *Nature Communications*, *5*, 3746.

Flanagan, J. M., & Wild, L. (2007). An epigenetic role for noncoding RNAs and intragenic DNA methylation. *Genome Biology*, *8*(6), 307.

Gelfman, S., Cohen, N., Yearim, A., & Ast, G. (2013). DNA-methylation effect on cotranscriptional splicing is dependent on GC architecture of the exon-intron structure. *Genome Research*, *23*(5), 789–99.

Hoivik, E. A., Bjanesoy, T. E., Mai, O., Okamoto, S., Minokoshi, Y., Shima, Y., … Bakke, M. (2011). DNA methylation of intronic enhancers directs tissue-specific expression of steroidogenic factor 1/adrenal 4 binding protein (SF-1/Ad4BP). *Endocrinology*, *152*(5), 2100–12.

Kazantseva, Y. A., Yarushkin, A. A., & Pustylnyak, V. O. (2013). Dichlorodiphenyltrichloroethane technical mixture regulates cell cycle and apoptosis genes through the activation of CAR and ERα in mouse livers. *Toxicology and Applied Pharmacology*, *271*(2), 137–43.

Kim, J. H., Sartor, M. A., Rozek, L. S., Faulk, C., Anderson, O. S., Jones, T. R., … Dolinoy, D. C. (2014). Perinatal bisphenol A exposure promotes dose-dependent alterations of the mouse methylome. *BMC Genomics*, *15*, 30.

Lau, M. Y., Han, H., Hu, J., & Ji, C. (2013). Association of cyclin D and estrogen receptor α36 with hepatocellular adenomas of female mice under chronic endoplasmic reticulum stress. *Journal of Gastroenterology and Hepatology*, *28*(3), 576–83.

Liu, W.-H., Yeh, S.-H., Lu, C.-C., Yu, S.-L., Chen, H.-Y., Lin, C.-Y., … Chen, P.-J. (2009). MicroRNA-18a prevents estrogen receptor-alpha expression, promoting proliferation of hepatocellular carcinoma cells. *Gastroenterology*, *136*(2), 683–93.

Manikkam, M., Guerrero-Bosagna, C., Tracey, R., Haque, M. M., & Skinner, M. K. (2012). Transgenerational actions of environmental compounds on reproductive disease and identification of epigenetic biomarkers of ancestral exposures. *PloS One*, *7*(2), e31901.

Maunakea, A. K., Nagarajan, R. P., Bilenky, M., Ballinger, T. J., D'Souza, C., Fouse, S. D., … Costello, J. F. (2010). Conserved role of intragenic DNA methylation in regulating alternative promoters. *Nature*, *466*(7303), 253–7.

Murphy, S. K., Adigun, A., Huang, Z., Overcash, F., Wang, F., Jirtle, R. L., … Hoyo, C. (2012). Gender-specific methylation differences in relation to prenatal exposure to cigarette smoke. *Gene*, *494*(1), 36–43.

Nahar, M. S., Liao, C., Kannan, K., & Dolinoy, D. C. (2013). Fetal liver bisphenol a concentrations and biotransformation gene expression reveal variable exposure and altered capacity for metabolism in humans. *Journal of Biochemical and Molecular Toxicology*, *27*(2), 116–23.

Phillips, J. M., Burgoon, L. D., & Goodman, J. I. (2009). Phenobarbital elicits unique, early changes in the expression of hepatic genes that affect critical pathways in tumor-prone B6C3F1 mice. *Toxicological Sciences : An Official Journal of the Society of Toxicology*, *109*(2), 193–205.

Prins, G. S., Hu, W.-Y., Shi, G.-B., Hu, D.-P., Majumdar, S., Li, G., … van Breemen, R. B. (2014). Bisphenol A promotes human prostate stem-progenitor cell self-renewal and increases in vivo carcinogenesis in human prostate epithelium. *Endocrinology*, *155*(3), 805–17.

Prins, G. S., Tang, W.-Y., Belmonte, J., & Ho, S.-M. (2008). Developmental exposure to bisphenol A increases prostate cancer susceptibility in adult rats: epigenetic mode of action is implicated. *Fertility and Sterility*, *89*(2 Suppl), e41.

Rademacher, K., Schröder, C., Kanber, D., Klein-Hitpass, L., Wallner, S., Zeschnigk, M., & Horsthemke, B. (2014). Evolutionary origin and methylation status of human intronic CpG islands that are not present in mouse. *Genome Biology and Evolution*, *6*(7), 1579–88.

Raggi, C., & Invernizzi, P. (2013). Methylation and liver cancer. *Clinics and Research in Hepatology and Gastroenterology*, *37*(6), 564–71.

Rauch, T. A., Wu, X., Zhong, X., Riggs, A. D., & Pfeifer, G. P. (2009). A human B cell methylome at 100-base pair resolution. *Proceedings of the National Academy of Sciences of the United States of America*, *106*(3), 671–8.

Rebouissou, S., Amessou, M., Couchy, G., Poussin, K., Imbeaud, S., Pilati, C., … Zucman-Rossi, J. (2009). Frequent in-frame somatic deletions activate gp130 in inflammatory hepatocellular tumours. *Nature*, *457*(7226), 200–4.

Rosell, R., Bertran-Alamillo, J., Molina, M. A., & Taron, M. (2009). IL-6/gp130/STAT3 signaling axis in cancer and the presence of in-frame gp130 somatic deletions in inflammatory hepatocellular tumors. *Future Oncology (London, England)*, *5*(3), 305–8.

Sandoval, J., Peiró-Chova, L., Pallardó, F. V, & García-Giménez, J. L. (2013). Epigenetic biomarkers in laboratory diagnostics: emerging approaches and opportunities. *Expert Review of Molecular Diagnostics*, *13*(5), 457–71.

Sekine, Y., Yamamoto, T., Yumioka, T., Imoto, S., Kojima, H., & Matsuda, T. (2004). Cross-talk between endocrine-disrupting chemicals and cytokine signaling through estrogen receptors. *Biochemical and Biophysical Research Communications*, *315*(3), 692–8.

Shi, L., Feng, Y., Lin, H., Ma, R., & Cai, X. (2014a). Role of estrogen in hepatocellular carcinoma: is inflammation the key? *Journal of Translational Medicine*, *12*(1), 93.

Shi, L., Feng, Y., Lin, H., Ma, R., & Cai, X. (2014b). Role of estrogen in hepatocellular carcinoma: is inflammation the key? *Journal of Translational Medicine*, *12*, 93.

Shukla, S., & Meeran, S. M. (2014). Epigenetics of cancer stem cells: Pathways and therapeutics. *Biochimica et Biophysica Acta*, *1840*(12), 3494–3502.

Umemura, A., Park, E. J., Taniguchi, K., Lee, J. H., Shalapour, S., Valasek, M. A., … Karin, M. (2014). Liver damage, inflammation, and enhanced tumorigenesis after persistent mTORC1 inhibition. *Cell Metabolism*, *20*(1), 133–44.

Vandenberg, L. N., Chahoud, I., Heindel, J. J., Padmanabhan, V., Paumgartten, F. J. R., & Schoenfelder, G. (2012). Urinary, circulating, and tissue biomonitoring studies indicate widespread exposure to bisphenol A. *Ciência & Saúde Coletiva*, *17*(2), 407–34.

Vandenberg, L. N., Ehrlich, S., Belcher, S. M., Ben-Jonathan, N., Dolinoy, D. C., Hugo, E. R., … vom Saal, F. S. (2013). Low dose effects of bisphenol A: An integrated review of in vitro, laboratory animal, and epidemiology studies. *Endocrine Disruptors*, *1*(1).

Waterland, R. A., & Jirtle, R. L. (2003). Transposable elements: targets for early nutritional effects on epigenetic gene regulation. *Molecular and Cellular Biology*, *23*(15), 5293–300.

Weinhouse, C., Anderson, O. S., Bergin, I. L., Vandenbergh, D. J., Gyekis, J. P., Dingman, M. A., … Dolinoy, D. C. (2014). Dose-dependent incidence of hepatic tumors in adult mice following perinatal exposure to bisphenol A. *Environmental Health Perspectives*, *122*(5), 485–91.

Weinhouse, C., Anderson, O. S., Jones, T. R., Kim, J., Liberman, S. A., Nahar, M. S., … Dolinoy, D. C. (2011). An expression microarray approach for the identification of metastable epialleles in the mouse genome. *Epigenetics : Official Journal of the DNA Methylation Society*, *6*(9).

Table 3.1 Post-natal day 22 (PND22) mouse liver samples (n=147) and 10-month mouse liver samples (n=78) for bisulfite sequencing.

Age	BPA dose (per kg maternal diet)	Total animals			Animals with hepatic tumors or pre-neoplastic lesions		
		Males	**Females**	**Total**	**Males**	**Females**	**Total**
PND22 mice	Control	17	20	37			
	50 ng	17	31	48			
	50 µg	12	10	22			
	50 mg	19	21	40			
	Total	65	82	147			
10-month mice	Control	10	9	19	2	0	
	50 ng	10	10	20	1	2	
	50 µg	11	10	21	3	2	
	50 mg	9	9	18	4	4	
	Total	40	38	78	10	8	18

Table 3.2 Candidate gene regions for bisulfite sequencing.

Candidate Gene	Species	Gene Coordinates	RefSeq Isoforms	Assay Coordinates	Assay Genomic Context	CpG island
Esr1	Mouse	Chr10: 5342780-5734495	1	Chr10: 5644941-5645340	Intron	No
ESR1	Human	Chr6: 152128814-152424408	3	Chr6: 152022101-152022700	Intron	No
Il-6st	Mouse	Chr13: 113254278-113297068	1	Chr13: 113294809-113295208	Exon	No
IL-6ST	Human	Chr5: 55230925-55290821	3	Chr5: 55255601-55256200	Intron	Yes
Stat3	Mouse	Chr11: 100748124-100800825	3	Chr11: 100766115-100766514	Exon, plus 100bp 5' intron and 150bp of 3' intron	Yes
STAT3	Human	Chr17: 40465343-40540513	3	Chr17: 4049190-40492500	Intron	Yes

Table 3.3 Primer sets for bisulfite sequencing.

Assay	Forward Primer	Reverse Primer	Product Size	T$_A$	Number of CpG sites
Esr1	5'-TTGTGTGATTTGGTTAGAATTTGAG-3'	5'- TTAAAAAACTCCCTAACACATTCCC-3'	348bp	59ºC	2
ESR1	5'-GGGAAAAGTTGTATTAAGTTGTATTGTTT-3'	5'-ACTACAACCTCCACCTCCTAAATTC-3'	434bp	59ºC	2
Il-6st	5'-TTTTTTATAGTTGGAGGATTTTGTG-3'	5'- AAACCATACTTCTCTAACAAACCCA-3'	301bp	59ºC	3
IL-6ST	5'-GGAGTATTTTTGGATAAGTTTTTTTGA-3'	5'-AACTCACACCTATAATCCCAATACTTT-3'	381bp	56ºC	7
Stat3	5'-GTTTAGGTAGATGTTGGGAGGGTT-3'	5'-TTCCAAACAAAACATTATAAATAAACTAAC-3'	148bp	56ºC	3
STAT3	5'-ATTAGTATTTGGGAAGGTTGAAGTG-3'	5'- TACAAACATACACCACCAAACTCAA-3'	324bp	64ºC	3

All forward primers contained the following 5' sequence tag: *aggaagagag*. All reverse primers contained the following 5' sequence tag: *cagtaatacgactcactatagggagaaggct*.

Table 3.4 Primer sets for mRNA expression analysis for *Stat3* and *STAT3* via qPCR.

Assay	Forward Primer	Reverse Primer
Stat3	5'- AGTTCAAGCACCTGACCCTT -3'	5'-TCAGTCACGATCAAGGAGGC-3'
B2m	5'-CCTTCAGCAAGGACTGGTCT-3'	5'- TCAGTCTCAGTGGGGGTGAA -3'
Gapdh	5'- CCGCATCTTCTTGTGCAGT-3'	5'-GGCAACAATCTCCACTTTGC-3'
STAT3	5'-GGGAAAAGTTGTATTAAGTTGTATTGTTT-3'	5'-ACTACAACCTCCACCTCCTAAATTC-3'
UBC	5'-GATCGCTGTGATCGTCACTT-3'	5'-TCTTTG CCTTGACATTCTCG-3'
GAPDH	5'-CATCAATGGAAATCCCATCA-3'	5'-GACTCCACGACGTACTCAGC-3'

Table 3.5 *Esr1* methylation in 10-month mouse livers by dose and tumor status

	Tumor				Non-tumor				P-value
		95% confidence interval					**95% confidence interval**		
Dose	**Estimate**	**Lower limit**	**Upper Limit**	**Dose**	**Estimate**	**Lower limit**	**Upper limit**		
Control	91.3	90.7	91.9	Control	91.67	91.3	92.1		0.56
50 ng	90.9	87.3	92.4	50 ng	91.0	90.3	91.6		0.95
50 μg	92.9	92.0	93.8	50 μg	92.2	91.6	92.9		0.51
50 mg	90.2	89.4	91.1	50 mg	91.7	91.0	92.5		0.15

Table 3.6 Site-specific *Esr1* methylation in 10-month mouse livers by dose

			95% confidence interval		P-value
CpG Site	**Dose**	**Estimate**	**Lower limit**	**Upper limit**	
Average methylation	Control	91.7	91.0	92.3	Reference
	50 ng	90.8	90.2	91.5	0.33
	50 μg	92.4	91.8	93.0	0.39
	50 mg	91.1	90.4	91.7	0.52
CpG site 1	Control	84.9	83.7	86.1	Reference
	50 ng	81.6	80.4	82.8	0.05
	50 μg	85.4	84.3	86.5	0.75
	50 mg	83.0	81.9	84.2	0.27
CpG site 2	Control	99.2	98.6	99.9	Reference
	50 ng	98.8	98.2	99.5	0.63
	50 μg	100.0	99.4	100.6	0.39
	50 mg	98.9	98.3	99.5	0.69

Table 3.7 Site-specific *Esr1* methylation in PND22 mouse livers by dose

| CpG Site | Dose | Estimate | 95% confidence interval | | P-value |
			Lower limit	Upper limit	
Average methylation	Control	81.8	77.8	85.9	Reference
	50 ng	90.7	86.9	94.4	0.11
	50 µg	91.4	86.6	96.2	0.13
	50 mg	91.1	87.4	94.9	0.10
CpG site 1	Control	75.6	71.4	79.7	Reference
	50 ng	68	79.9	87.5	0.15
	50 µg	83.7	78.8	88.6	0.20
	50 mg	83.7	79.9	87.5	0.14
CpG site 2	Control	88.4	84.3	92.5	Reference
	50 ng	97.7	93.9	101.4	0.10
	50 µg	98.8	94.0	103.7	0.10
	50 mg	98.3	94.5	102.0	0.08

Table 3.8 *ESR1* methylation in human fetal livers by total BPA tertiles

CpG Site	Dose	Estimate	95% confidence interval Lower limit	95% confidence interval Upper limit	Comparison	P-value
Average methylation	Low BPA	58.9	58.1	61.6		
					Low BPA vs. Medium BPA	0.14
	Medium BPA	56.4	54.8	57.9		
					Medium BPA vs. High BPA	0.39
	High BPA	58.2	56.6	59.7		
					Low BPA vs. High BPA	0.45
	Continuous					0.71
CpG site 1	Low BPA	48.1	45.1	51.2		
					Low BPA vs. Medium BPA	0.28
	Medium BPA	43.7	41.0	46.3		
					Medium BPA vs. High BPA	0.28
	High BPA	47.7	45.1	50.3		
					Low BPA vs. High BPA	0.91
CpG site 2	Low BPA	71.6	69.8	73.3		
					Low BPA vs. Medium BPA	0.16
	Medium BPA	68.2	66.7	69.7		
					Medium BPA vs. High BPA	0.42
	High BPA	69.6	68.2	71.1		
					Low BPA vs. High BPA	0.49

Table 3.9 *ESR1* methylation in human fetal livers by free BPA tertiles

CpG Site	Dose	Estimate	95% confidence interval		Comparison	P-value
			Lower limit	Upper limit		
Average methylation	Low BPA	59.9	58.2	61.7		
					Low BPA vs. Medium BPA	0.04
	Medium BPA	55.4	53.9	56.9		
					Medium BPA vs. High BPA	0.06
	High BPA	59.2	57.7	60.6		
					Low BPA vs. High BPA	0.72
	Continuous					0.67
CpG site 1	Low BPA	48.2	45.2	51.2		
					Low BPA vs. Medium BPA	0.21
	Medium BPA	43.0	40.4	45.6		
					Medium BPA vs. High BPA	0.16
	High BPA	48.3	45.7	50.9		
					Low BPA vs. High BPA	0.98
CpG site 2	Low BPA	71.6	69.9	73.3		
					Low BPA vs. Medium BPA	0.05
	Medium BPA	67.1	65.7	68.5		
					Medium BPA vs. High BPA	0.08
	High BPA	70.7	69.3	72.1		
					Low BPA vs. High BPA	0.69

Table 3.10 *Il-6st* methylation in 10-month mouse livers by dose and tumor status

Tumor				Non-tumor				P-value
		95% confidence interval				95% confidence interval		
Dose	Estimate	Lower limit	Upper Limit	Dose	Estimate	Lower limit	Upper limit	
Control	83.0	81.0	84.9	Control	81.6	80.6	82.6	0.47
50 ng	84.5	82.5	86.5	50 ng	80.9	79.9	82.0	0.08
50 µg	82.1	80.7	83.4	50 µg	81.4	80.4	82.4	0.61
50 mg	80.4	79.2	81.6	50 mg	83.1	81.9	84.2	0.03

Table 3.11 Site-specific *Il-6st* methylation in 10-month mouse livers by dose

CpG Site	Dose	Estimate	95% confidence interval		P-value
			Lower limit	Upper limit	
Average methylation	Control	81.9	80.8	82.9	Reference
	50 ng	81.4	80.3	82.4	0.59
	50 µg	81.6	80.6	82.5	0.74
	50 mg	81.9	80.9	82.9	1.0
CpG site 1	Control	78.2	74.6	81.9	Reference
	50 ng	79.3	75.5	83.0	0.59
	50 µg	71.4	68.2	74.7	0.17
	50 mg	76.5	72.9	80.0	0.73
CpG site 2	Control	87.7	86.8	88.6	Reference
	50 ng	86.6	85.7	87.5	0.37
	50 µg	88.3	87.6	89.1	0.57
	50 mg	87.9	87.0	88.7	0.90
CpG site 3	Control	81.5	78.4	84.7	Reference
	50 ng	84.8	81.5	88.0	0.47
	50 µg	78.1	75.2	80.9	0.41
	50 mg	81.7	78.6	84.7	0.97

Table 3.12 Site-specific *Il-6st* methylation in PND22 mouse livers by dose

| CpG Site | Dose | Estimate | 95% confidence interval | | P-value |
			Lower limit	Upper limit	
Average methylation	Control	83.2	82.3	84.1	Reference
	50 ng	81.7	81.9	83.4	0.58
	50 µg	83.5	82.6	84.5	0.76
	50 mg	82.3	81.5	83.1	0.37
CpG site 1	Control	71.9	69.0	74.8	Reference
	50 ng	75.4	73.4	77.4	0.32
	50 µg	81.1	77.7	84.4	0.04
	50 mg	77.0	74.7	79.4	0.16
CpG site 2	Control	90.8	89.9	91.6	Reference
	50 ng	90.3	89.6	90.9	0.66
	50 µg	90.3	89.4	91.3	0.75
	50 mg	89.1	88.4	89.8	0.12
CpG site 3	Control	84.0	81.5	86.5	Reference
	50 ng	79.3	77.5	81.1	0.04
	50 µg	83.2	80.3	86.1	0.85
	50 mg	84.9	82.8	86.9	0.78

Table 3.13 *IL-6ST* methylation in human fetal livers by total BPA tertiles

CpG Site	Dose	Estimate	95% confidence interval		Comparison	P-value
			Lower limit	Upper limit		
Average methylation	Low BPA	88.7	88.2	89.2		
					Low BPA vs. Medium BPA	0.99
	Medium BPA	88.7	88.2	89.2		
					Medium BPA vs. High BPA	0.97
	High BPA	88.7	88.2	89.2		
					Low BPA vs. High BPA	0.98
	Continuous					0.33
CpG site 1	Low BPA	82.4	81.5	83.4		
					Low BPA vs. Medium BPA	0.85
	Medium BPA	82.7	81.7	83.7		
					Medium BPA vs. High BPA	0.24
	High BPA	81.0	80.0	82.0		
					Low BPA vs. High BPA	0.31
CpG site 2	Low BPA	87.5	87.0	88.1		
					Low BPA vs. Medium BPA	1.0
	Medium BPA	87.5	86.9	88.1		
					Medium BPA vs. High BPA	0.39
	High BPA	88.3	87.7	88.8		
					Low BPA vs. High BPA	0.38
CpG site 3	Low BPA	97.3	96.7	97.9		
					Low BPA vs. Medium BPA	0.59
	Medium BPA	96.8	96.2	97.4		

					Medium BPA vs. High BPA	0.17
	High BPA	98.0	97.4	98.6		
					Low BPA vs. High BPA	0.40
CpG site 4	Low BPA	81.2	79.1	83.2		
					Low BPA vs. Medium BPA	0.21
	Medium BPA	85.0	82.8	87.2		
					Medium BPA vs. High BPA	0.13
	High BPA	80.2	78.1	82.3		
					Low BPA vs. High BPA	0.74
CpG site 5	Low BPA	91.7	90.6	92.8		
					Low BPA vs. Medium BPA	0.32
	Medium BPA	93.3	92.1	94.5		
					Medium BPA vs. High BPA	0.02
	High BPA	89.2	88.1	90.3		
					Low BPA vs. High BPA	0.13
CpG site 6	Low BPA	95.0	94.2	95.8		
					Low BPA vs. Medium BPA	0.62
	Medium BPA	95.5	94.7	96.4		
					Medium BPA vs. High BPA	0.10
	High BPA	93.7	92.9	94.4		
					Low BPA vs. High BPA	0.23
CpG site 7	Low BPA	88.0	86.6	89.3		
					Low BPA vs. Medium BPA	0.61
	Medium BPA	87.0	85.5	88.4		
					Medium BPA vs. High BPA	0.01
	High BPA	81.7	80.3	83.0		
					Low BPA vs. High BPA	<0.01

Table 3.14 *IL-6ST* methylation in human fetal livers by free BPA tertiles

CpG Site	Dose	Estimate	95% confidence interval		Comparison	P-value
			Lower limit	Upper limit		
Average methylation	Low BPA	88.7	88.2	89.2		
					Low BPA vs. Medium BPA	0.76
	Medium BPA	88.6	88.1	89.0		
					Medium BPA vs. High BPA	0.52
	High BPA	88.8	88.4	89.3		
					Low BPA vs. High BPA	0.76
	Continuous					0.59
CpG site 1	Low BPA	82.4	81.5	83.4		
					Low BPA vs. Medium BPA	0.93
	Medium BPA	82.3	81.3	83.3		
					Medium BPA vs. High BPA	0.52
	High BPA	81.4	80.4	82.4		
					Low BPA vs. High BPA	0.45
CpG site 2	Low BPA	87.6	87.0	88.1		
					Low BPA vs. Medium BPA	0.65
	Medium BPA	87.9	87.3	88.6		
					Medium BPA vs. High BPA	0.96
	High BPA	87.9	87.3	88.5		
					Low BPA vs. High BPA	0.67
CpG site 3	Low BPA	97.3	96.7	97.9		
					Low BPA vs. Medium BPA	0.39
	Medium BPA	96.6	96.0	97.2		
					Medium BPA vs. High BPA	0.05
	High BPA	98.2	97.7	98.8		
					Low BPA vs. High BPA	0.25

CpG site 4	Low BPA	81.2	79.1	83.3			
					Low BPA vs. Medium BPA	0.30	
	Medium BPA	84.4	82.2	86.6			
					Medium BPA vs. High BPA	0.25	
	High BPA	80.8	78.6	82.9			
					Low BPA vs. High BPA	0.89	
CpG site 5	Low BPA	91.7	90.5	92.8			
					Low BPA vs. Medium BPA	0.48	
	Medium BPA	92.9	91.7	94.1			
					Medium BPA vs. High BPA	0.06	
	High BPA	89.6	88.5	90.8			
					Low BPA vs. High BPA	0.22	
CpG site 6	Low BPA	95.0	94.2	95.8			
					Low BPA vs. Medium BPA	0.97	
	Medium BPA	94.9	94.1	95.8			
					Medium BPA vs. High BPA	0.54	
	High BPA	94.2	93.4	95.0			
					Low BPA vs. High BPA	0.51	
CpG site 7	Low BPA	88.0	86.6	89.4			
					Low BPA vs. Medium BPA	0.34	
	Medium BPA	86.0	84.5	87.5			
					Medium BPA vs. High BPA	0.02	
	High BPA	82.6	81.1	84.0			
					Low BPA vs. High BPA	0.01	

Table 3.15 *Stat3* methylation in 10-month mouse livers by dose and tumor status

	Tumor				Non-tumor			P-value
		95% confidence interval				95% confidence interval		
Dose	Estimate	Lower limit	Upper Limit	Dose	Estimate	Lower limit	Upper limit	
Control	69.0	64.9	73.0	Control	74.3	72.9	75.7	0.22
50 ng	73.1	69.1	77.2	50 ng	77.0	75.5	78.4	0.38
50 μg	70.5	68.2	72.9	50 μg	77.8	76.4	79.3	0.01
50 mg	72.5	70.4	74.5	50 mg	77.3	75.4	79.1	0.08

Table 3.16 Site-specific *Stat3* methylation in 10-month mouse livers by dose

CpG Site	Dose	Estimate	95% confidence interval		P-value
			Lower limit	Upper limit	
Average methylation	Control	71.4	70.0	72.9	Reference
	50 ng	74.3	72.8	75.7	0.12
	50 μg	74.5	73.2	75.7	0.09
	50 mg	74.8	73.4	76.1	0.08
CpG site 1	Control	72.5	70.7	74.3	Reference
	50 ng	76.5	74.7	78.4	0.09
	50 μg	75.3	73.7	76.9	0.22
	50 mg	76.1	74.3	77.8	0.15
CpG site 2	Control	69.9	68.4	71.5	Reference
	50 ng	73.5	72.0	75.1	0.08
	50 μg	73.9	72.5	75.3	0.05
	50 mg	74.2	72.8	75.7	0.04
CpG site 3	Control	71.2	72.4	74.9	Reference
	50 ng	74.0	72.5	75.5	0.15
	50 μg	73.7	72.4	74.9	0.18
	50 mg	74.1	72.8	75.5	0.14

Table 3.17 Site-specific *Stat3* methylation in mouse livers by dose

CpG Site	Dose	Estimate	95% confidence interval		P-value
			Lower limit	Upper limit	
Average methylation	Control	86.7	86.1	87.3	Reference
	50 ng	85.8	85.2	86.3	0.24
	50 µg	83.5	82.7	84.3	<0.01
	50 mg	84.7	84.1	85.2	0.01
CpG site 1	Control	87.9	87.2	88.6	Reference
	50 ng	87.0	86.4	87.6	0.36
	50 µg	85.3	84.4	82.3	0.03
	50 mg	86.6	86.5	87.3	0.19
CpG site 2	Control	86.8	86.0	87.5	Reference
	50 ng	85.4	84.8	86.0	0.01
	50 µg	84.7	83.8	85.6	0.07
	50 mg	83.3	82.7	84.0	<0.01
CpG site 3	Control	85.5	84.7	86.3	Reference
	50 ng	84.8	84.2	85.5	<0.01
	50 µg	80.7	79.7	81.7	0.01
	50 mg	83.9	83.1	84.6	<0.01

Table 3.18 *STAT3* methylation in human fetal livers by total BPA tertiles

CpG Site	Dose	Estimate	95% confidence interval		Comparison	P-value
			Lower limit	Upper limit		
Average methylation	Low BPA	81.7	80.6	82.9		
					Low BPA vs. Medium BPA	0.77
	Medium BPA	82.0	80.8	83.1		
					Medium BPA vs. High BPA	0.87
	High BPA	82.1	80.9	83.2		
					Low BPA vs. High BPA	0.64
	Continuous					0.01
CpG site 1	Low BPA	64.4	58.8	70.0		
					Low BPA vs. Medium BPA	0.27
	Medium BPA	55.6	50.0	61.1		
					Medium BPA vs. High BPA	0.18
	High BPA	66.1	60.9	71.3		
					Low BPA vs. High BPA	0.83
CpG site 2	Low BPA	89.6	88.8	90.4		
					Low BPA vs. Medium BPA	0.14
	Medium BPA	91.3	90.5	92.0		
					Medium BPA vs. High BPA	0.60
	High BPA	90.7	90.1	91.4		
					Low BPA vs. High BPA	0.28
CpG site 3	Low BPA	93.2	92.6	93.7		
					Low BPA vs. Medium BPA	0.81
	Medium BPA	93.0	92.5	93.5		
					Medium BPA vs. High BPA	0.68
	High BPA	93.3	92.8	93.7		
					Low BPA vs. High BPA	0.90

Table 3.19 *STAT3* methylation in human fetal livers by free BPA tertiles

CpG Site	Dose	Estimate	Lower limit	Upper limit	Comparison	P-value
			95% confidence interval		**Comparison**	**P-value**
Average methylation	Low BPA	81.8	80.6	82.9		
					Low BPA vs. Medium BPA	0.80
	Medium BPA	81.6	80.5	82.8		
					Medium BPA vs. High BPA	0.26
	High BPA	82.3	81.2	83.5		
					Low BPA vs. High BPA	0.43
	Continuous					0.02
CpG site 1	Low BPA	64.4	58.8	70.1		
					Low BPA vs. Medium BPA	0.41
	Medium BPA	57.8	52.2	63.5		
					Medium BPA vs. High BPA	0.43
	High BPA	63.9	58.7	69.2		
					Low BPA vs. High BPA	0.95
CpG site 2	Low BPA	89.6	88.9	90.4		
					Low BPA vs. Medium BPA	0.17
	Medium BPA	91.2	90.4	91.9		
					Medium BPA vs. High BPA	0.26
	High BPA	90.8	90.1	91.5		
					Low BPA vs. High BPA	0.73
CpG site 3	Low BPA	93.2	92.7	93.7		
					Low BPA vs. Medium BPA	0.43
	Medium BPA	92.6	92.1	93.1		
					Medium BPA vs. High BPA	0.60
	High BPA	93.6	93.1	94.0		
					Low BPA vs. High BPA	0.15

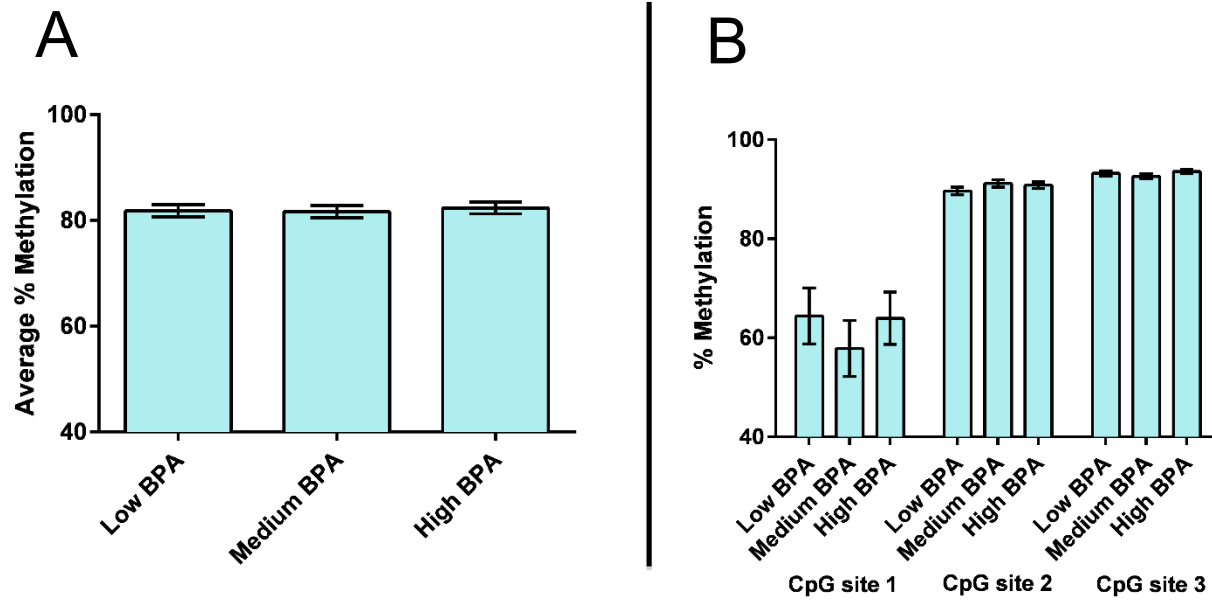**Figure 3.1 *Stat3* Methylation in 10-month Mouse Livers by Dose and Tumor Status**
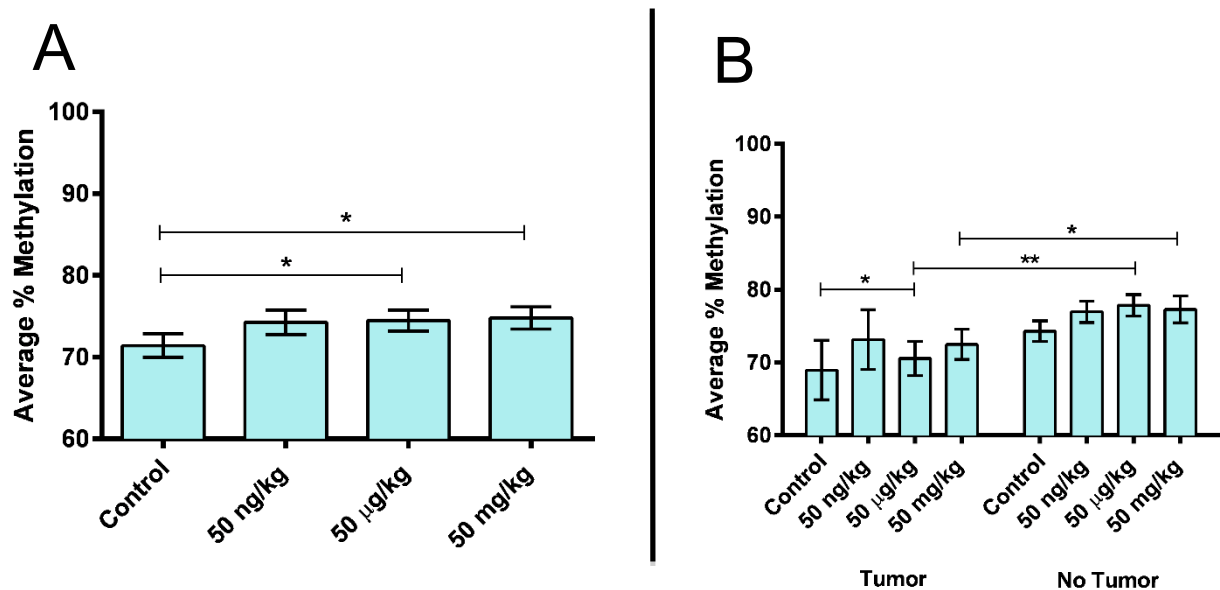
(A) Average percent DNA methylation at *Stat3* by dose group in 10-month mice perinatally exposed to 50 ng (n=20), 50 ug (n=21) or 50 mg (n=18) BPA/kg maternal diet or a phytoestrogen-free control diet (n=19). (B) Percent DNA methylation at *Stat3* by tumor status in 10-month mice perinatally exposed to 50 ng (n=20), 50 ug (n=21) or 50 mg (n=18) BPA/kg maternal diet or a phytoestrogen-free control diet (n=19). *p<0.1, **p<0.05

Figure 3.2 Site-specific *Stat3* Methylation in 10-month Mouse Livers by Dose
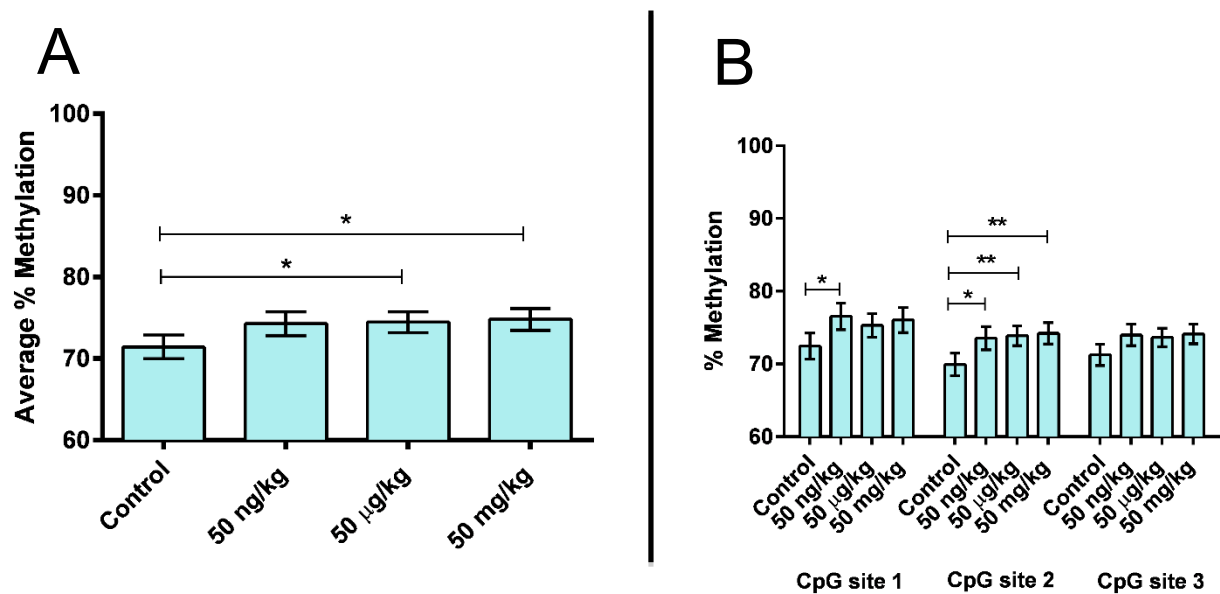
(A) Average percent DNA methylation at *Stat3* by dose group in 10-month mice perinatally exposed to 50 ng (n=20), 50 ug (n=21) or 50 mg (n=18) BPA/kg maternal diet or a phytoestrogen-free control diet (n=19). (B) Percent DNA methylation at *Stat3* by CpG site in 10-month mice perinatally exposed to 50 ng (n=20), 50 ug (n=21) or 50 mg (n=18) BPA/kg maternal diet or a phytoestrogen-free control diet (n=19). *p<0.1, **p<0.05

Figure 3.3 Site-specific *Stat3* Methylation in PND22 Mouse Livers by Dose
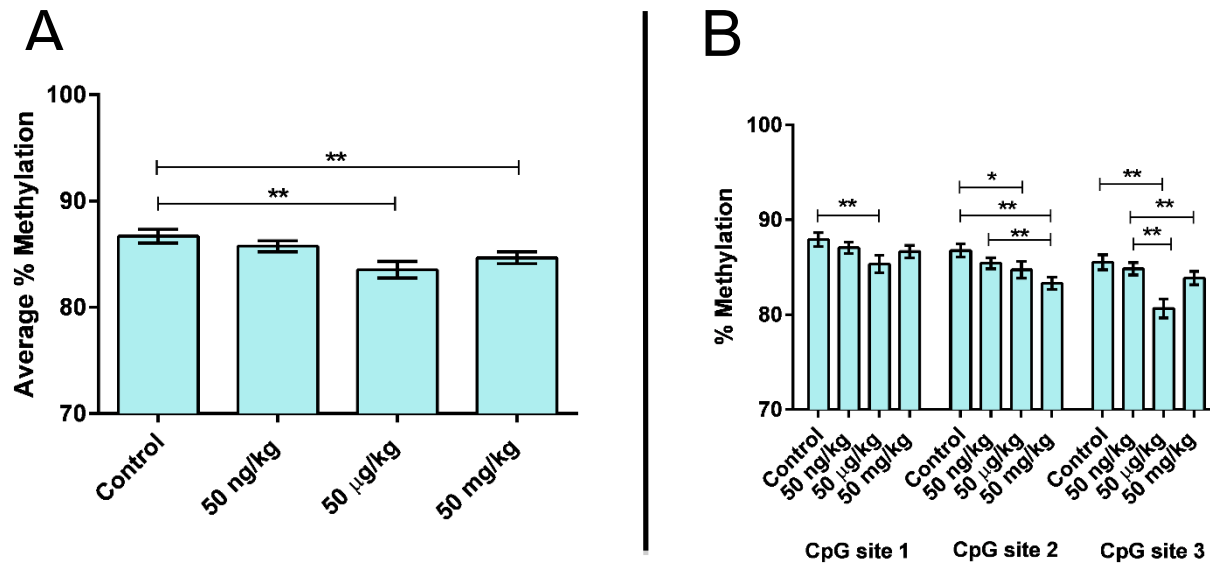
(A) Average percent DNA methylation at *Stat3* by dose group in post-natal day 22 (PND22) mice perinatally exposed to 50 ng (n=48), 50 ug (n=22) or 50 mg (n=40) BPA/kg maternal diet or a phytoestrogen-free control diet (n=37). (B) Percent DNA methylation at *Stat3* by CpG site in PND22 mice perinatally exposed to 50 ng (n=48), 50 ug (n=22) or 50 mg (n=40) BPA/kg maternal diet or a phytoestrogen-free control diet (n=37). *p<0.1, **p<0.05

Figure 3.4 *STAT3* Methylation in Human Fetal Livers by Total BPA Tertiles
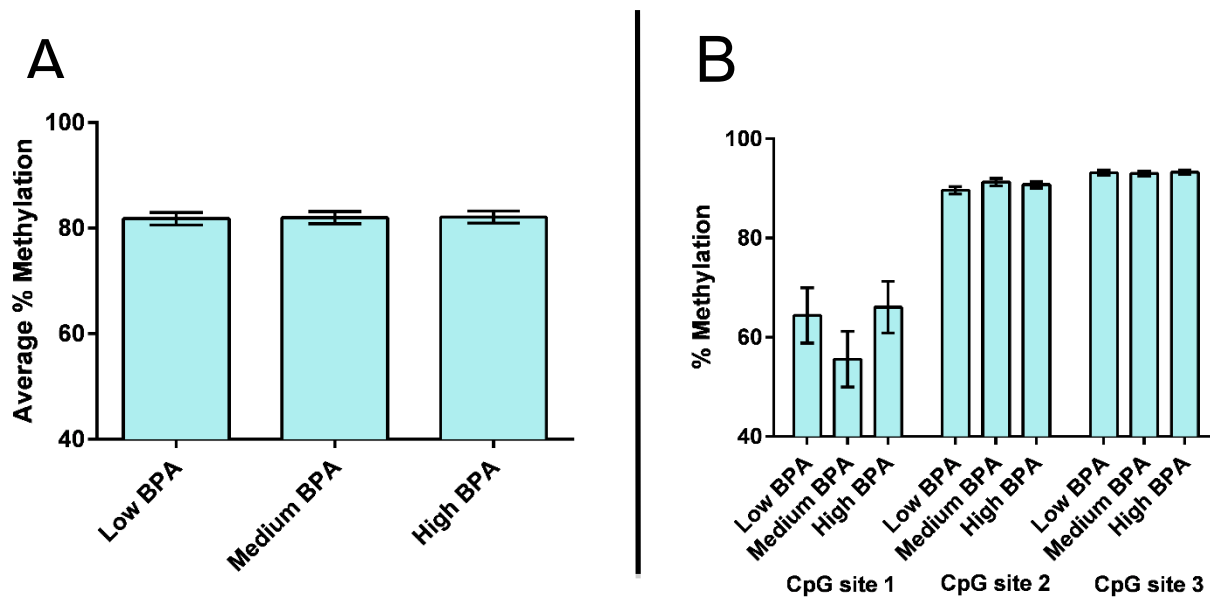
(A) Average percent DNA methylation at *STAT3* by dose group in human fetal liver samples (n=50) by tertile of liver tissue total BPA. (B) Percent DNA methylation at *STAT3* by dose group and CpG site in human fetal liver samples (n=50) by tertile of liver tissue total BPA.

Figure 3.5 *STAT3* Methylation in Human Fetal Livers by Free BPA Tertiles

(A) Average percent DNA methylation at *STAT3* by dose group in human fetal liver samples (n=50) by tertile of liver tissue free BPA.

(B) Percent DNA methylation at *STAT3* by dose group and CpG site in human fetal liver samples (n=50) by tertile of liver tissue free BPA.

Figure 3.6 *STAT3* Methylation in Human Fetal Livers by Continuous Total BPA

Average percent DNA methylation at *STAT3* by dose group in human fetal liver samples (n=50) by continuous liver tissue total BPA.
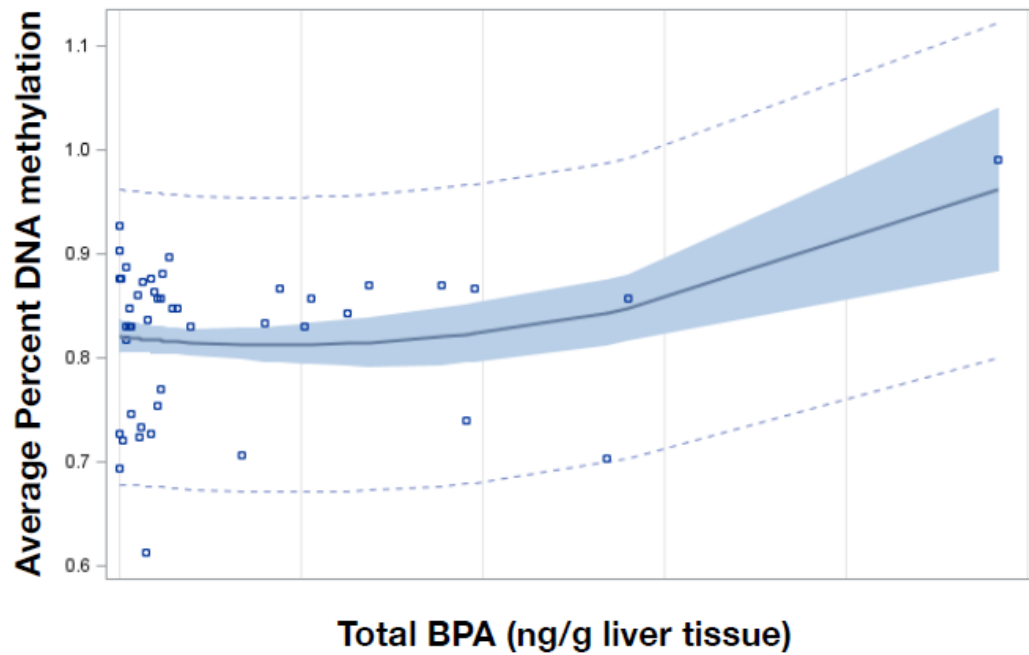
Figure 3.7 *STAT3* Methylation in Human Fetal Livers by Continuous Free BPA
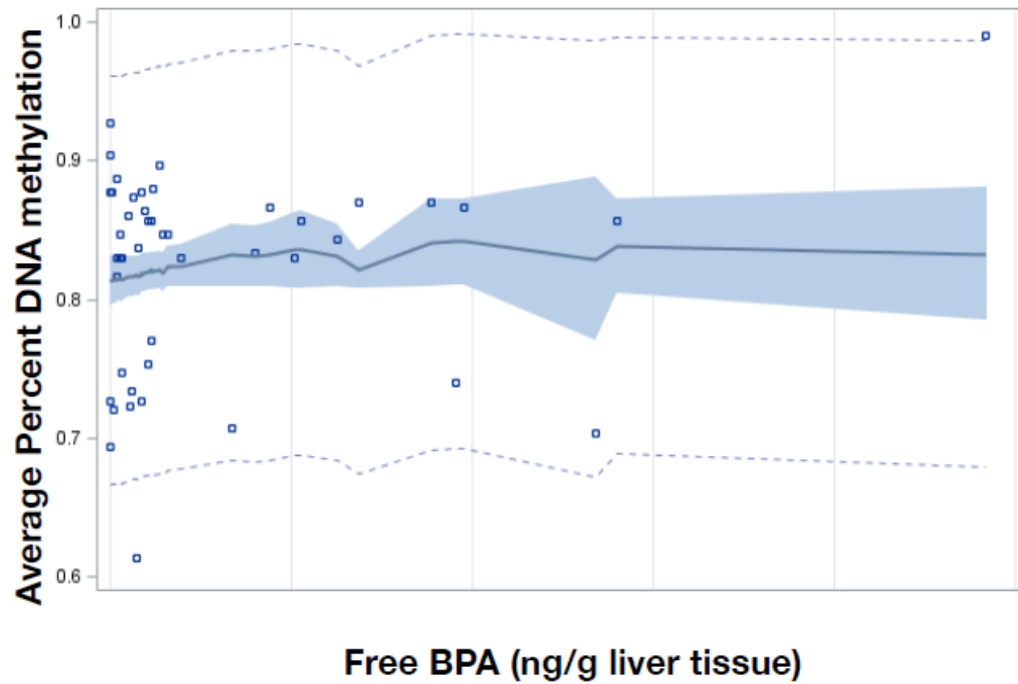
Average percent DNA methylation at *STAT3* by dose group in human fetal liver samples (n=50) by continuous liver tissue free BPA.

Figure 3.8 *Stat3* Expression in 10-month Mouse Livers by Dose and Tumor Status
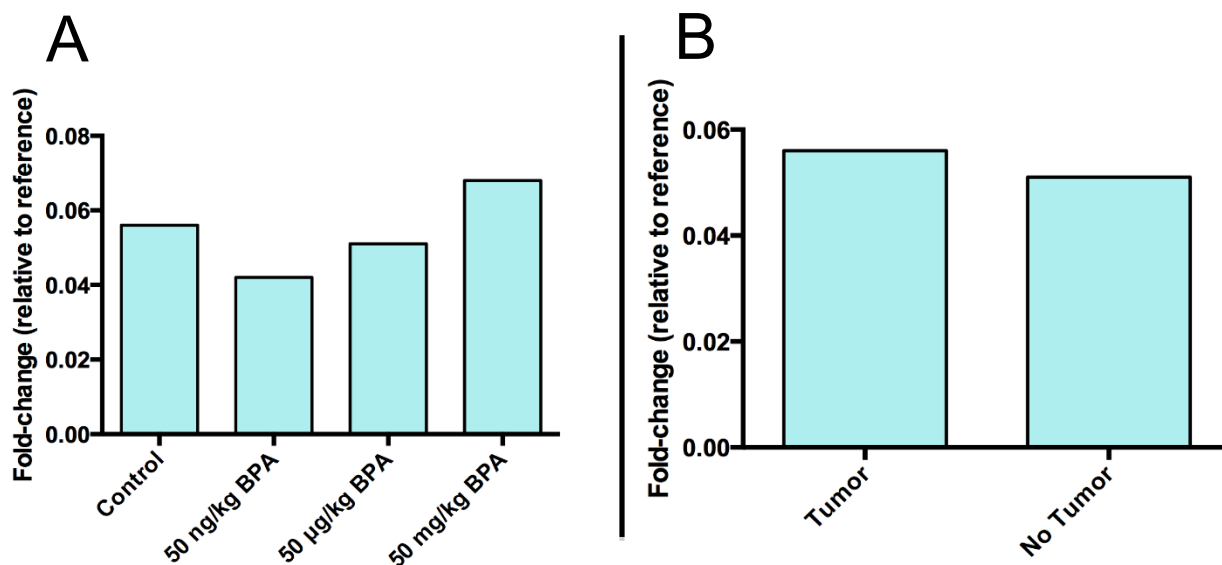
(A) Fold-change of *Stat3* transcript level by dose group in 10-month mice perinatally exposed to 50 ng (n=20), 50 ug (n=21) or 50 mg (n=18) BPA/kg maternal diet or a phytoestrogen-free control diet (n=19). (B) Fold-change of *Stat3* transcript level *Stat3* by tumor status in 10-month mice perinatally exposed to 50 ng (n=20), 50 ug (n=21) or 50 mg (n=18) BPA/kg maternal diet or a phytoestrogen-free control diet (n=19).

Figure 3.9 *Stat3* Expression in PND22 Mouse Livers by Dose
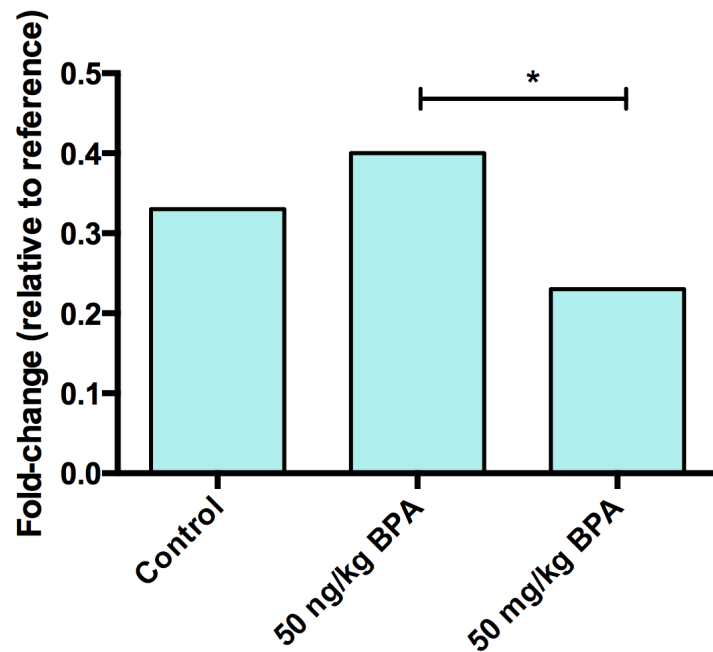
Fold-change of *Stat3* transcript level at *Stat3* by dose group in post-natal day 22 (PND22) mice perinatally exposed to 50 ng (n=48), 50 ug (n=22) or 50 mg (n=40) BPA/kg maternal diet or a phytoestrogen-free control diet (n=37). *p<0.1

Figure 3.10 *STAT3* Expression in Human Fetal Livers by Continuous Total BPA
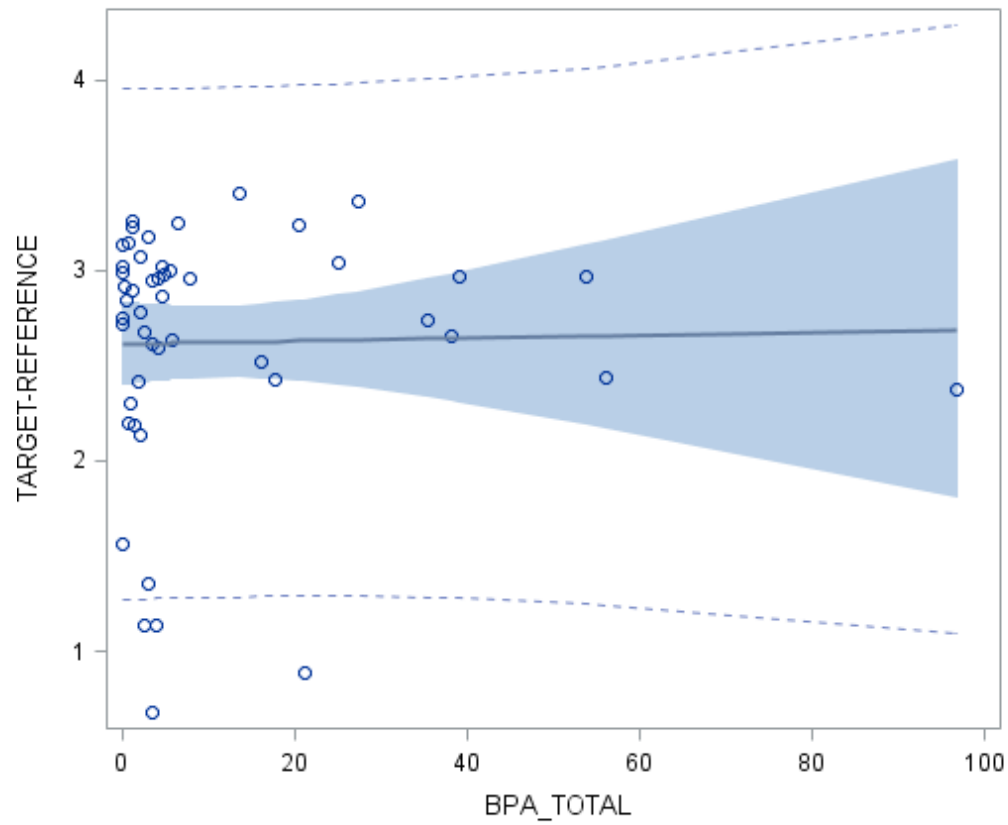
Fold-change of *STAT3* transcript level in human fetal livers (n=50) by continuous total BPA.

Figure 3.11 *STAT3* Expression in Human Fetal Livers by Continuous Free BPA
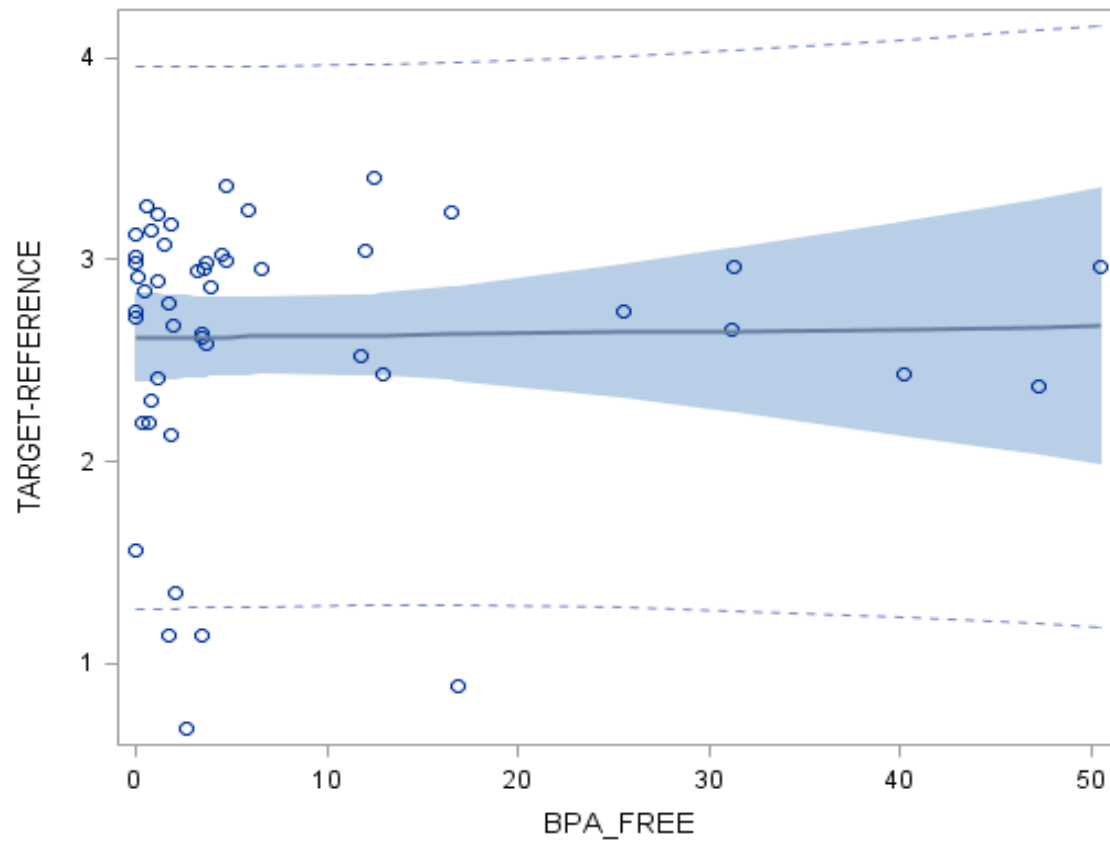
Fold-change of *STAT3* transcript level in human fetal livers (n=50) by continuous free BPA

CHAPTER 4

Epigenome-wide DNA Methylation Analysis Implicates Neuronal and Inflammatory Signaling Pathways in Hepatic Tumorigenesis in Mice Perinatally Exposed to Bisphenol A

4.1   Abstract

Developmental exposure to the endocrine-active compound bisphenol A (BPA) has been linked to epigenotoxic and potential carcinogenic effects in rodent prostate and mammary glands. We previously reported a dose-dependent increase in hepatic tumors in 10-month mice perinatally exposed to one of three doses of BPA (50 ng, 50 μg, or 50 mg BPA/kg chow). These tumors represent early-onset disease and lack classical sexual dimorphism in incidence. Here, we investigate epigenome-wide DNA methylation profiles at gene promoters associated with BPA exposure and disease via methylcytosine enrichment in 10-month mice with and without liver tumors. Pathway enrichment analysis revealed mouse and human genes linked to BPA exposure related to intracellular Jak/STAT and MAPK signaling pathways likely linked to sexual dimorphism of HCC. Taken together, these findings are indicators of the relevance of the hepatic tumor phenotype seen in BPA-exposed mice to human health. This work demonstrates that epigenome-wide discovery experiments in animal models are effective tools for identification and understanding of paralagous epimutations salient to human disease.

4.2   Introduction

Bisphenol A (BPA) is a high production volume monomer used in the manufacture of polycarbonate plastics and other consumer products that has been implicated as an endocrine disruptor, due to its ability to bind both canonical and non-canonical estrogen receptors (Welshons, et al., 2006). Biomonitoring studies routinely detect levels of BPA in urine in > 90% of adults in the United States, indicating that exposure to BPA is widespread (Calafat et al., 2008).

In Chapter 2, we reported a dose-dependent increase in hepatic tumors in 10-month mice that were perinatally exposed to one of three doses of the endocrine disruptor bisphenol A (BPA) (Weinhouse et al., 2014). Notably, no statistically significant relationship between liver tumors and BPA exposure in adult mice and rats was seen in the 1982 National Toxicology Program Carcinogenicity Bioassay on BPA, the last regulatory evaluation of BPA's carcinogenicity, despite employing doses 200-20,000 times higher than those used in our study, supporting the importance of exposure timing (NTP 1982). The liver tumors in our study were evident at 10-months of age, which represents early onset disease in mice, and did not exhibit the classical sexual dimorphism in incidence (Weinhouse et al., 2014), which is largely accepted to result from the protective, anti-inflammatory effect of endogenous estrogen in human and rodent females (Shi et al., 2014). We observed only a proliferative response in exposed animals with hepatic tumors, with no evidence of fibrosis or necrosis, indicating that cellular proliferation was not due to a regenerative response to tissue injury (Weinhouse et al., 2014). BPA has been linked to proliferative tissue changes in rat mammary glands (Acevedo et al., 2013) and to frank prostate cancer in mice with human prostate stem cell xenografts supplemented with sex steroid hormones to mimic human male aging (Prins et al., 2014). However, frank tumors have not been

definitively linked to BPA exposure in humans, indicating a need for focusing *in vivo* animal experiments on outcomes with clear translational relevance to human exposure and disease. Animal studies are well poised to interrogate health outcomes of chemical exposures whose systematic administration would be unethical in humans, as well as to investigate whole organism questions that require tissues not easily obtainable from human study participants or that require tight control of experimental conditions, as in the case of environmentally ubiquitous endocrine disruptors.

Exposure to the endocrine disruptor bisphenol A (BPA) has previously been shown to alter DNA methylation at the coat-color linked A^{vy} (viable yellow *Agouti*) metastable epiallele in mice (Anderson et al., 2012a; Dolinoy et al., 2007) indicating that perinatal BPA exposure may dysregulate the epigenome. Several studies have identified epigenetic alterations at specific genes linked to BPA dose and tissue alterations (Avissar-Whiting et al., 2010; Greathouse et al., 2012), supporting the hypothesis that epigenetic changes may mediate the relationship between early life BPA exposure and adult health outcomes. BPA has been linked to dysregulation of potential mediators of tumorigenesis in reproductive estrogen target organs in rodents and humans. Rats injected neonatally with 2.4 μg BPA per day showed hypermethylation of both nuclear estrogen receptors (Doshi et al., 2011), which have been linked to xenoestrogen-induced human breast cancer (Pupo et al., 2012). Promoter hypomethylation and concomitant transcriptional upregulation at developmental transcription factor *Hoxa10* following BPA exposure in mice and human mammary carcinoma cells led to increased ERE-driven gene expression following increased ERα activity (Bromer et al, 2010). Global epigenomic regulators are altered by BPA exposure, as well, including histone methyltransferase *Ezh2* (Doherty et al.,

2010), maintenance DNA methyltransferases *Dnmt3a* and *Dnmt3b* (Doshi et al., 2011) and methyl binding proteins *Mbd2* and *Mbd4* (Tang et al., 2012).

To date, few studies have investigated alterations to epigenetic marks across the genome following BPA exposure. Epigenome-wide approaches, including microarray platforms and deep sequencing methods, assess genome-wide profiles of epigenetic marks of interest, such as DNA methylation, and are thus effective as discovery tools for assessing large-scale, pathway level changes. Dhimolea et al. observed epigenome-wide alterations in DNA methylation at post-natal day 21 in Wistar-Furth rats exposed perinatally to BPA, although the majority of transcriptional changes did not occur until post-natal day 50 (2014). Kim et al. reported regions of altered methylation in CpG island shores, rather than CpG islands, and noted alterations in pathways associated with metabolism and stimulus response (2014). However, to our knowledge, no study to date has utilized an epigenome-wide platform to assess pathway level changes associated with both BPA exposure and the presence of an adverse health effect in rodents or humans.

Here, we demonstrate the effectiveness of an epigenome-wide discovery approach for characterization of pathway-level dynamics linked to liver tumors in BPA-exposed animals described in Chapter 2. These results indicate that, when coupled with data analysis focused on translation to human health, experimental animal data can guide future mechanistic and epidemiological work and thereby effectively inform human disease prevention and treatment.

4.3   Materials and Methods

4.3.1   Mouse Liver Samples

Liver tissues utilized in this chapter include wild-type *a/a* 10-month mice with frank liver tumors that were perinatally exposed to BPA via maternal diet and maintained on phytoestrogen-free control diet from weaning at PND22 until 10 months of age (n=16 offspring; n=4 male and

n=4 female offspring exposed to "low BPA," or 50 ng or 50 µg BPA/kg maternal diet; n=4 male

and n=4 female offspring exposed to "high BPA," or 50 mg BPA/kg maternal diet), as well as

wild-type *a/a* control mice (n=6 offspring; n=3 male and n=3 female) that were maintained on

phytoestrogen-free control diet for the duration of the study, as described in Chapters 1 and 2.

Mice were obtained from a colony generated by backcrossing C3H/HeJ mice carrying the viable

yellow *Agouti* (A^{vy}) allele with C57BL/6J mice, followed by >200 generations of sibling mating

(Waterland & Jirtle, 2003). The A^{vy} strain is isogenic (Waterland & Jirtle, 2003) and has been

empirically confirmed to be genetically 93% C57BL/6J (Weinhouse et al., 2014). Offspring of

virgin wild-type (*a/a*) females and heterozygous (A^{vy}/a) males were exposed during gestation and

lactation to one of three doses of BPA (50 ng, 50 µg, or 50 mg/kg maternal diet) or to a

phytoestrogen-free control diet, as previously described (Weinhouse et al., 2014). This mating

scheme produced approximately 50% wild-type (*a/a*) offspring and approximately 50%

heterozygous (A^{vy}/a) offspring. The majority of A^{vy}/a mice were euthanized on post-natal day

(PND) 22 (Anderson et al., 2012b). A subset of wild-type (*a/a*) mice (approximately 1 male and

1 female per litter for each BPA diet group) were then housed with a same-sex A^{vy}/a sibling and

fed the standard phytoestrogen-free control diet until they were euthanized at 10 months of age,

as described by Anderson et al. (Anderson et al., 2013). During dissection of both PND22 and

10-month animals, liver tissue was collected and flash frozen in liquid nitrogen. Liver tissue

from 10-month animals was evaluated for histopathologic lesions, including benign and

malignant tumors, as previously described (Weinhouse et al., 2014). Liver tissue measurements

for free and conjugated (glucuronidated and sulfated) BPA in PND22 mouse liver samples

(Anderson et al., 2012a) have confirmed liver BPA levels within the range of reported human

environmental exposures (Vandenberg et al., 2012).

4.3.2 DNA Isolation

Total genomic DNA was isolated from 10-month liver tissue (n=22) using a standard phenol-chloroform extraction method. Briefly, approximately 10-15 mg of liver tissue was homogenized for three 20-second pulses at 15 Hz (TissueLyser, Qiagen) in 540 µl of lysis buffer (buffer ATL, Qiagen) and incubated overnight at 50 ºC with 60 µl Proteinase K. Lysate was then incubated with 12 µl RNase A for 10 minutes at 37 ºC. The DNA-containing aqueous phase was extracted twice with 600 µl phenol-chloroform-isoamyl alcohol, followed by a single extraction with 600 µl chloroform, using Phase Gel Lock tubes (5 Prime, Gaithersburg, Maryland). 50 µl 3M sodium acetate was added to decanted aqueous phase. DNA was precipitated once with 1 mL of 100% ethanol and twice with 1 mL of 75% ethanol. Pellets were air dried and resuspended in 50 µl Tris-EDTA buffer during 2-hour incubation at 60 ºC with frequent mixing.

4.3.3 DNA Fragmentation

Genomic DNA was sheared to fragment sizes ranging from 200 to 1000 bp using manufacturer's instructions on an Episonic 1100 series sonicator (Farmingdale, NY). Briefly, 17 µg of DNA was divided into two volumes of 8.5 µg in separate PCR tubes and was sonicated in a polycarbonate plastic tube rack with a total process time of 15 minutes (15 second on and 30 second off cycles, amplitude of 18) in 8-20 ºC water. Water was monitored and cooled with sonicator cooling system every 5 minutes of process time. Fragment sizes for each sample were confirmed with ~1 µg DNA via gel electrophoresis. One sonicated aliquot per sample was enriched for methylated DNA, as described below. Matching sample aliquots were reserved as genomic input for co-hybridization with enriched fractions to microarrays.

4.3.4 Enrichment and Whole Genome Amplification of Methylated DNA

Methylated DNA fragments from one sonication aliquot per sample were enriched for

methylcytosine using methyl-CpG binding domain-based capture (MBD-Cap) with the EpiMark

Methylated DNA Enrichment Kit (New England BioLabs, Ipswich, Massachusetts). MBD

protein domains most efficiently bind DNA that is both CpG dense and highly methylated,

compared to restriction enzyme or methyl-cytosine antibody techniques, which may identify sites

of single methylated CpGs (Laird, 2010, Thorne et al., 2009). Antibody or methyl binding-

protein affinity enrichment of methylated DNA is inefficient, but highly specific and dose-

dependent. The level of enrichment is positively correlated with the number of methylated

cytosines on a given DNA fragment. Methyl-CpG binding proteins preferentially enrich for

regions of high CpG density and high DNA methylation; enrichment is most efficient when at

least >2 CpG sites are present and regions with CpG density <2% are not enriched efficiently.

5mC antibodies are better able to enrich for fragments with a single methylated CpG site, but

requires single stranded DNA for 5mC recognition (MBD-Cap uses dsDNA) and is more user-

and reagent-dependent than MBD-cap. Both bisulfite-treated DNA microarrays and methyl

antibody-based enrichment microarrays yield high-resolution (quantitative) data on a small

number of CpG sites (one CpG site per probe). Methyl-CpG binding protein-based enrichment

microarrays yield lower resolution (relative) data on larger regions of DNA that are likely to be

highly CpG dense and highly methylated. Sequences that are not sufficiently CpG dense or

methylated will be missed by this technique (Laird, 2010, Thorne et al., 2009).

The EpiMark kit contains a fusion protein (MBD-Fc) containing the highly conserved

methyl binding domain (MBD) of human MBD2 protein fused to the Fc tail of human IgG.

MBD-Fc proteins and paramagnetic protein A beads were incubated for 15 minutes at room

temperature, allowing Fc domains to couple with protein A beads, and washed twice.

Fragmented genomic DNA was added to MBD-Fc/bead mixture, rotated at room temperature for 20 minutes, and washed three times to discard unbound DNA. Captured methylated DNA was eluted with 100 µl of DNase-free water during a 15-minute incubation at 65 ºC. Residual unmethylated DNA fractions were reserved for downstream enrichment testing via qPCR. In order to obtain sufficient DNA for microarray hybridization, 10 ng of captured methylated DNA was amplified using GenomePlex Complete Whole Genome Amplification Kit (Sigma-Aldrich, St. Louis, Missouri).

4.3.5 Methylated DNA Enrichment Quality Assessment

Quality assessment for methylated DNA enrichment was performed via qPCR of two methylated regions at *Xist* and *H19* loci used as positive control probes on the microarray platform used in this study. Chromosomal coordinates of control probes were obtained directly from microarray manufacturers (Roche NimbleGen Inc., Madison, Wisconsin) and qPCR assays were designed to capture *Xist* and *H19* positive control probe sequences. Approximately 60 ng each of genomic input sonicated DNA (diluted 1:10), unmethylated DNA from uncaptured fraction reserved after enrichment step (diluted 1:10), and WGA enriched DNA (diluted 1:100) was analyzed for relative enrichment of fragments containing control probe sequences. Quantitative PCR was performed in duplicate 25 µl reactions using SYBR Green Master Mix (Qiagen Inc., Valencia, California), 0.25 pmol forward and reverse primers, and 60 ng input DNA from above, under the following reaction conditions: 95 ºC for 3 minutes, followed by 39 cycles of 10 seconds at 95 ºC, 62 ºC for 30 seconds, 72 ºC for 10 seconds, with a final incremental temperature decrease from 95 ºC for melt curve analysis to confirm product uniqueness. The average threshold cycle ($C(t)$) from duplicate reactions was calculated using CFX Manager Version1.6 software (Bio-Rad). A minimum of 10-fold enrichment of positive

control regions in methylated fraction over genomic fraction was confirmed for each sample prior to sample hybridization to microarrays.

4.3.6. Hybridization and Array Scanning

Several hybridization comparisons are possible on enrichment microarrays, given three fractions of DNA for each sample: input DNA (unenriched), umethylated fraction (non-captured DNA from enrichment step), and methylated fraction (enriched.) Methylated or unmethylated fractions from two different samples may be directly compared in a single array. Methylated samples may each be compared to a common reference sample used for all arrays for indirect comparison. This method is used for differential methylation analysis (DMH), but it is difficult to find an appropriate reference sample and the methylation status of the reference sample is often unknown. Individual samples may be co-hybridized to single arrays, as well, including comparisons of unmethylated or methylated fraction to input or methylated fraction to unmethylated fraction. In this experiment, we compared methylated fractions to input for individual samples. The log-ratios of signal intensities generated by this approach are easier to interpret than those in the other approaches and each sample represents its own reference. However, methylated and unmethylated sequences are not equally detectable for this setup - the dynamic range of the log-ratios is restricted and positive log-ratios are more difficult to detect than negative log-ratios. This range is less restricted when comparing methylated to unmethylated fractions (Laird, 2010, Thorne et al., 2009).

In order to compare methylated fractions to genomic input, per the hybridization scheme described above, experimental enriched and genomic input fractions for each sample were labeled with Cy5 and Cy3, respectively, with NimbleGen Dual-Color Labeling Kit (Roche NimbleGen, Madison, Wisconsin) following instructions in the NimbleGen Array User Guide

(Nimblegen Array User Guide *DNA Methylation Arrays*, Version 7.2). Labeled fractions were pooled and co-hybridized to Roche NimbleGen Mouse DNA Methylation 3x720K CpG Island Plus RefSeq Promoter Arrays for 16-20 hours. These promoter methylation tiling arrays contain three subarrays, each containing 720,000 probes that scan 15,980 CpG islands in 20,404 murine gene promoters. Probe tiling ranges from 2,960bp upstream to 740bp downstream of transcription start sites. Probes range in length from 50-75bp with median probe spacing of 100bp. Following hybridization, arrays were washed and scanned using a 2 µm resolution NimbleGen MS 200 Microarray Scanner (Dr. Thomas Glover, Department of Human Genetics, University of Michigan). All arrays were run by a single individual in two batches during January and March, months in which humidity and ozone levels were fairly consistently low.

4.3.7. Bioinformatics Pipeline

We used the R packages *Ringo* and *limma*. Raw intensity values were background corrected using the *norm+exp-offset* method (to prevent loss of data that is common using background subtraction), and then quantile normalized across all samples. Quantile normalization was performed on untransformed intensity values, since the normalization has been reported to be more effective on intensity values as compared to $\log_2$ signal intensity ratios. Regression models were run on normalized $\log_2$ signal intensity ratios.

4.3.7.1. Implications of Enrichment Method for Analysis

Cancer-related DNA methylation changes have been reported most commonly as global hypomethylation and promoter CpG island (CGI) hypermethylation. As MBD-Cap enrichment efficiently enriches for highly methylated, CpG dense fragments, $\log_2$ signal intensity ratios >1 likely represent promoter hypermethylation. Although $\log_2$ ratios =1 may be interpreted as "no methylation change", there are likely to be regions of "no methylation change" that appear

hypomethylated ($\log_2$ ratio <1), because regions of sparse methylation and low CpG density are poorly enriched with this method, and because differences between the methylated and input fractions are more difficult to distinguish than differences between methylated and unmethylated fractions (Adriaens et al., 2012; Laird, 2010). Probe cross-hybridization and noise in the signal contribute to this ambiguous cutoff for change (Adriaens et al., 2012; Laird, 2010).

As regions of highly methylated, CpG-dense DNA are most likely to be enriched by MBD-Cap, high intensity signal in the red (Cy5) channel, reading enriched methylated DNA signal, is likely to correlate with both high CpG density and high percent methylation levels. Further, this approach provides information on larger regions of DNA but less quantitatively than bisulfite treated-DNA arrays, which provide single CpG site data at higher resolution and assume similarity of methylation at neighboring sites (Adriaens et al., 2012; Laird, 2010).

4.3.7.2. Background Correction

Array images were uploaded to NimbleGen DEVA software (version 2.3) and aligned using an automated alignment grid function. Raw signal intensities for each channel were exported using the software report function and analyzed in R version 3.1.1. Raw array files provide intensity data on R (red channel, Cy5) and G (green channel, Cy3) foreground (overall spot) intensities and R_b and G_b background (ambient signal) intensities (Smyth & Speed, 2003; Sun, Huang, Yan, Huang, & Lin, 2011). Background may arise from non-specific sample binding across the whole array or cross-hybridization of probes that increases local background (Sun et al 2011). As log-intensities of spike-in controls are systematically underestimated with no background correction in expression microarrays (Thorne et al., 2009), and in light of the difficulty in detecting positive log-ratios in our hybridization setup, a background correction step was included. Traditional subtraction background correction, which involves subtracting

background intensities from foreground intensities, may lead to missing log-ratios if corrected values are negative and high variability in low intensity spots. Variance stabilizing normalization (vsn), which stabilizes variability over the intensity range to reduce variability of low intensity ratios, was avoided because the method requires the assumption of static variability over intensity range, which is unlikely to be true in methylation datasets, and because the method normalizes both channels together, possibly removing real signal (Huber et al., 2002). Therefore, in this analysis, background correction was performed using the *normexp+offset* method. In this method, a normal-exponential convolution model is applied to the local background and foreground in red and green channels separately, and a small positive offset (k=50) is added to both channels to reduce the variance of low intensity log values, a common problem in cDNA expression microarrays. Although high variance of low intensity log values is not evident in MA plots of non-normalized log2 ratios in this dataset, the offset is unlikely to introduce bias.

4.3.7.3. Within-Array Normalization

Within array normalization methods are intended to remove bias due to differences in dye incorporation due to quenching ("dye bias") and spatial bias across each array (Smyth & Speed, 2003). In older arrays that are spotted with print tips, print tip groups may introduce spatial bias (Smyth & Speed, 2003). In newer, *in situ* synthesized arrays, spatial bias is largely due to differences in starting sample material amount and uneven sample hybridization or washing (Thorne et al., 2009). However, the main assumptions required by most within array normalization methods are not likely valid in this experiment and their use may remove true signal. Most methods assume that the majority of probes are not differentially regulated (methylated); that the number of upregulated (hypermethylated) probes will equal the number of downregulated (hypomethylated) probes; and that differentially regulated probes will be evenly

spread across the signal range (ie, not intensity-dependent) (Laird, 2010; Reimers, 2010; Sun et al., 2011). It can be difficult to determine whether differences are due to dye bias or to real differences in global methylation, particularly with samples that are expected to differ significantly, such as tumor and non-tumor samples. Thus, it may not be possible to adjust for dye-bias and spatial differences without removing true biological signal (Laird, 2010; Reimers, 2010; Sun et al., 2011). Misapplied loess normalization may not only remove true signal but also introduce systematic bias (Adriaens et al., 2012; Laird, 2010; Reimers, 2010; Sun et al., 2011). Therefore, no within array normalization method was incorporated in this analysis.

4.3.7.4. Across-Array Normalization

Across array normalization methods are meant to make arrays more comparable to one another and to remove differences that may arise in individual array preparation or handling (Adriaens et al., 2012; Smyth & Speed, 2003). However, if arrays are biologically different from one another, care must be taken not to erase these differences (Adriaens et al., 2012; Smyth & Speed, 2003). Scaling methods, such as Tukey's biweight mean scaling, compress data from all arrays on to a set scale makes them more comparable to one another. However, if the true median log-ratio for one array is biologically less than zero and biologically greater than zero on a second array, scaling these arrays to center them on zero would remove true across-array differences in methylation. Quantile normalization was employed for across array normalization in this analysis. Quantile normalization equalizes the distribution across arrays to increase array comparability. Although, this normalization method may erase differences in range and variability between tumor samples and. non-tumor samples, performing quantile normalization in each dose group individually erroneously assumes similarity among tumor samples within a dose group. Quantile normalization was performed on untransformed intensity values, since the

normalization has been reported to be more effective on intensity values as compared to $\log_2$ signal intensity ratios.

4.3.7.5. Linear Regression Models

Two individual predictors (binary dose variable and binary sex variable) were tested in separate models for each of three pair-wise dose group comparisons (low BPA vs. control; high BPA vs. control; high BPA vs. low BPA), for a total of six dose group models. Additionally, two individual predictors (binary tumor status variable and binary sex variable) were tested in separate models for the pair-wise comparison of tumor vs. non-tumor (a combination of low BPA and high BPA groups, in this experiment) samples.

4.3.8. Identification and Validation of Top Differentially Methylated Probes

4.3.8.1. Bisulfite Sequencing of Probes for Technical Validation

Genomic DNA was isolated from 10-month mouse liver tissue samples run on microarrays (n=22) using buffer ATL, proteinase K, and RNase A (QIAGEN Inc., Valencia, CA), followed by phenol-chloroform extraction and ethanol precipitation. DNA quality and concentration was assessed using a ND1000 spectrophotometer (NanoDrop Technology, Wilmington, DL). Quantitative DNA methylation patterns were analyzed via sodium bisulfite treatment followed by sequencing using Sequenom EpiTYPER MassARRAY technology in 5' gene promoter regions containing differentially methylated probes with the lowest p-values (top hits) for each of four analysis comparisons (β = ratio of enriched to input signal): *Lce1m* (tumor vs. non-tumor; β=0.641, p=7.11E-6), *Shmt2* (high BPA vs. low BPA; β=3.162, p=2.22E-7), *Foxp2* (low BPA vs. control; β=0.383, p=4.6E-6), and *Ift46* (high BPA vs. control; β=3.181, p=2.17E-5). Sodium bisulfite treatment was performed using the QIAGEN EpiTect Bisulfite Kit (QIAGEN) with approximately 1 µg input genomic DNA. EpiTYPER assays were designed

using the Sequenom EpiDesigner tool (www.epidesigner.com) and top hit gene primer sets were assessed for unique products in the bisulfite-converted mouse and human genomes using the BiSearch ePCR tool (http://bisearch.enzim.hu). PCR was carried out in 25 µl reactions using approximately 50 ng of bisulfite-converted DNA, HotStarTaq master mix (QIAGEN Inc., Valencia, CA) and forward and reverse (0.1 pmol each) primers under the following conditions: 15 minutes at 95ºC, 40 cycles of (30 seconds at 94ºC, 30 seconds at annealing temperature (T_A), 1 minute at 72ºC), 10 minutes at 72ºC.

The third most significant probe in the tumor vs. non-tumor comparison was chosen for validation, because the first two did not contain CpG sites and were not within CpG islands, with adjacent regions of high CpG density. Primer sequences for bisulfite sequencing of microarray top hits are listed in **Table 4.1**.

4.3.8.2. Data Analysis for Technical Validation

Dose- and tumor-dependent DNA methylation changes in 10-month mice with tumors, as compared to 10-month control mice without tumors, were assessed using repeated measures mixed models (PROC MIXED), with individual CpG sites defined as repeated measures, in order to account for lack of independence of multiple CpG sites at a single locus within an individual animal (**Table 4.2**). One model was run per candidate gene, including four predictors: repeated CpG site, dichotomous tumor, dichotomous sex, and ordinal dose. Fixed effects of the dependent variable assessed associations between dose and tumor status with average methylation at a locus. Dose was coded as an ordinal variable for all administered doses (control=0, 50 ng BPA/kg maternal diet=1, 50 µg BPA/kg maternal diet=2, and 50 mg BPA/kg maternal diet=3). In order to directly validate microarray results, three contrast statements were included to closely mimic the comparisons in the regression models run on the microarray data

("low BPA," or an average of effects of the two lowest doses, as compared to control; "high

BPA," or the highest dose, as compared to control, and "high BPA," or the highest dose, as

compared to "low BPA", or an average of the effects of the two lowest doses). The tumor vs.

non-tumor comparison was directly tested with a dichotomous tumor variable. All models

contained a random intercept to cluster data by litter. In the model testing DNA methylation at

Ift46 (4 CpG sites in the assay), an unstructured variance-covariance matrix was computed from

the data (option *type=un*), in agreement with data from Chapter 2 and prior studies indicating

site-specific basal methylation and lability. In models testing DNA methylation at *Foxp2*, *Shmt2*,

and *Lce1m*, loci with large numbers of CpG sites, an unstructured variance-covariance matrix

could not be computed and empirical standard errors were instead calculated (option *empirical*).

All statistical analyses were performed in SAS v9.4 (Cary, NC).

4.3.9. Pathway and GO Term Enrichment Analysis

Complete probe lists with p-values and β values (normalized ratios of enriched to input

signal intensities) for each of four comparisons were uploaded to the LRpath web tool for

pathway (BioCarta, KEGG, Panther, EHMN, and pFAM) and GO terms (GO Biological

Processes, GO Molecular Function, and GO Cellular Component) enrichment analyses. LRpath

is a tool that tests for gene sets, or concepts, with significantly higher significance values than

expected at random using logistic regression, allowing data to remain on a continuous scale and

thus increasing statistical power to detect enrichment (Sartor et al., 2009). Probes were analyzed

as individual probes, rather than aggregated into larger windows of sequence or collapsed by

gene promoter, in order to retain high resolution of the tiling array platform and to detect region-

specific changes that may be masked by analysis of larger, smoothed windows. Histograms of

number of probes per gene in full probe list and limited to probes p<0.001 show similar

distributions, confirming that significant probe lists were not biased towards genes with high probe counts.

An agnostic exploration of GO terms (**Table 4.3**) and pathway terms (**Table 4.4**) with FDR values <0.1 were first assessed for evidence of statistically significant changes in pathways or cellular processes linked to BPA exposure and HCC. A hypothesis-driven approach investigating the influence of Jak/Stat and Mapk signaling pathways was pursued, as well. First, all pathway concepts related to Jak/Stat and Mapk signaling with p-values>0.05 in each of four comparisons were identified. Unique mouse microarray gene IDs in selected concepts related to Jak/Stat (70 mouse gene IDs) and Mapk (110 mouse gene IDs) across all four dose comparisons were annotated with gene names and descriptions using NCBI's Batch Entrez tool (http://www.ncbi.nlm.nih.gov/sites/batchentrez). To assess relevance of these results to human pathway response to BPA exposure, genes within human JAK/STAT (61 human gene IDs) and MAPK (177 human gene IDs) signaling pathways known to be altered by BPA were downloaded from The Comparative Toxicogenomics Database (CTD; http://ctdbase.org/) and compared to mouse microarray gene IDs. Gene set overlaps in these pathways are listed in **Tables 4.5** and **4.6** and shown visually in **Figures 4.1-4.4**. Gene set overlaps were overlaid onto KEGG pathways using the KEGG Pathway Mapper tool (http://www.genome.jp/kegg/pathway.html).

4.4. Results

Regression models tested methylation status at probes at 5' gene promoters across the epigenome via four pair-wise comparisons: 1) animals with tumors (n=16; n=8 males and n=8 females) as compared to animals without tumors (n=6; n=3 males and n=3 females); 2) animals exposed to low BPA (n=8; n=4 males and n=4 females) as compared to control animals (n=6; n=3 males and n=3 females); 3) animals exposed to high BPA (n=8; n=4 males and n=4 females)

as compared to control animals; and 4) animals exposed to high BPA as compared to those exposed to low BPA. In this analysis, all animals exposed to BPA also presented with hepatic tumors; therefore, the tumor versus non-tumor comparison is equivalent to the low and high BPA groups together compared to the control group. Mice with hepatic tumors showed 12,822 (1.8%) probes with differential methylation as compared to non-tumor animals at $p<0.01$ (lowest FDR value 0.53), of which 8,656 (67.5%) probes were hypomethylated (lowest signal intensity ratio=0.20) and 4,166 (32.5%) probes were hypermethylated (highest intensity ratio=5.3). Mice perinatally exposed to low BPA resulted in 3,752 (0.52%) probes with $p<0.01$ as compared to control animals (lowest FDR 0.84), of which 2,242 (59.8%) were hypomethylated (lowest signal intensity ratio=0.15) and 1,510 (40.2%) probes were hypermethylated (highest intensity ratio=7.2). High BPA-exposed animals presented with 9,649 (1.3%) probes with $p<0.01$ as compared to control animals (lowest FDR=0.63), with 6,467 (67%) hypomethylated probes (lowest intensity ratio=0.26) and 3,182 (33%) hypermethylated probes (highest intensity ratio=6.7). Finally, high BPA-exposed mice resulted in 7,308 (1.0%) probes with $p<0.01$ as compared to mice exposed to low BPA ($p<0.01$, lowest FDR=0.16), with 2,545 (34.8%) probes showing hypomethylation (lowest intensity ratio=0.31) and 4,763 (65.2%) probes showing hypermethylation (highest intensity ratio=8.7).

4.4.1. Identification and Validation of Top Differentially Methylated Probes

Technical validation of the microarray platform used in this study was performed via bisulfite sequencing of 5' gene promoter regions containing differentially methylated probes with the lowest p-values (top hits) for each of four analysis comparisons (β = ratio of enriched to input signal): 1) *Lce1m* (tumor vs. non-tumor; β=0.64, p=7.1E-6), 2) *Foxp2* (low BPA vs. control; β=0.38, p=4.6E-6), 3) *Ift46* (high BPA vs. control; β=3.2, p=2.2E-5) and 4) *Shmt2* (high

BPA vs. low BPA; β=3.2, p=2.2E-7). The third most significant probe set in the tumor vs. non-tumor comparison was chosen for validation, because the first two significant probe sets did not contain CpG sites and were not within CpG islands, with adjacent regions of high CpG density.

All four candidates displayed dose- or tumor-dependent methylation changes, and the directionality of change matched the direction of change indicated by each candidate probe's β value, or ratio of enriched to input signal intensities (**Table 4.2**). Promoter percent DNA methylation at *Lce1m* (tumor vs. non-tumor; β=0.641, p=7.11E-6 on microarray) showed no statistically significant relationship with tumor status (p=0.77), but did show a relationship with dose (p<0.0001). Promoter percent DNA methylation at *Foxp2* (low BPA vs. control; β=0.383, p=4.6E-6 on microarray) showed a statistically significant relationship with tumor status (0.8% hypomethylation, p=0.02) and marginally statistically significant association with high BPA as compared to control (0.7% hypomethylation, p=0.08). Percent DNA methylation at *Ift46* (high BPA vs. control; β=3.181, p=2.17E-5 on microarray) showed no statistically significant association with tumor status (p=0.61) but a relationship with dose was evident (p=<0.0001). Percent DNA methylation at *Shmt2* (high BPA vs. low BPA; β=3.162, p=2.22E-7 on microarray) showed no statistically significant relationship with tumor status (p=0.73) but did show a relationship with dose (p=<0.0001).

4.4.2. Gene Ontology Term Enrichment

Given that so few individual probes were significantly different among dose groups or by tumor status after correction for multiple testing, we decided to test for groups of genes significantly enriched with differential methylation using Gene Ontology terms, which can greatly increase the power to detect significant changes or trends (Ashburner et al., 2000). We tested for enriched GO terms in four comparisons: tumor vs. no tumor, low BPA vs. control, high

BPA vs control, and high BPA vs. low BPA. Thirty-three GO terms were enriched in animals with tumors as compared to animals without tumors (FDR<0.1) (**Table 4.3**). Genes in all 33 of the significant biological processes were hypermethylated, except two: *positive regulation of cell matrix adhesion* (p=5.1E-5, FDR=0.05) and *regulation of the force of heart contraction* (p=0.00072, FDR=0.064). The majority of these terms (n=27) were involved in morphogenesis or development (including *hepaticobiliary system development,* p=1.0E-5, FDR=0.0035; and *organ morphogenesis,* p=4.0E-4, FDR=0.046). The most significant GO term was *middle ear morphogenesis,* which contained 5 genes (out of 11) with a change in methylation and demonstrated a hypermethylation pattern (p=1.9E-8, FDR=4.6E-5). These five genes appeared 10 or 11 times each associated with the 33 GO terms on this list, indicating a high degree of overlap in these processes. Six GO terms related to epigenomic alteration displayed promoter hypermethylation in this comparison, as well (*demethylation*, p=0.00019, FDR=0.03; *histone modification*, p=2.9E-4, FDR=0.040; *covalent chromatin modification*, p=2.46E-4, FDR=0.038; *positive regulation of DNA repair*, p=3.7E-4, FDR=0.046; and *one-carbon metabolic process,* p=0.0017, FDR=0.11). The *demethylation* GO term contained eight genes, including CYP450 enzymes *Cyp3a11*, *Cyp3a16*, *Cyp3a44*, and three lysine-specific demethylases. The one-carbon metabolic process GO term contained 31 genes, including mitochondrial *serine hydroxymethyltransferase 2* (*Shmt2*) and *methionine adenosyltransferase I α* (*Mat1a*), which catalyzes the biosynthesis of methyl donor S-adenosylmethionine (Rountree et al., 2008).

Four GO terms were significant in the low BPA vs. control comparison (**Table 4.3**). Three terms that refer primarily to cellular transport were hypermethylated, including *Golgi to plasma membrane transport,* p=1.2E-5, FDR=0.03; *macromolecule transmembrane transporter activity*, p=1.4E-4, FDR=0.04; and *protein transmembrane transporter activity*, p=1.4E-4,

FDR=0.04. The remaining term, *NADP or NADPH binding* (p=5.3E-4, FDR=0.099), was

hypomethylated, and may be broadly related to the redox state of the cells investigated.

The high BPA vs. control comparison showed seven significant GO terms (**Table 4.3**),

including two terms related to transcription factor binding to DNA (*sequence specific DNA

binding*, p=1.5E-4, FDR=0.043; *sequence specific DNA binding transcription factor activity*,

p=2.6E-4, FDR=0.048) and two terms related to activity of ligases that form carbon-sulfur bonds

(*acid-thiol ligase activity*, p=5.1E-5, FDR=0.029, *ligase activity, forming carbon-sulfur bonds*,

p=4.02E-4, FDR=0.056). The remaining three terms refer to membrane-bound proteins (*extrinsic

to membrane*, p=3.15E-5, FDR=0.0061; *heterotrimeric G-protein complex*, p=3.27E-5,

FDR=0.0061; *extrinsic to plasma membrane,* p=3.2E-4, FDR=0.040). The remaining

comparison, high BPA vs. low BPA, showed the same seven significant GO terms listed above

for the high BPA vs. control comparison (**Table 4.3**).

4.4.3. Pathway Enrichment

Testing for pathways enriched with differential methylation revealed a predominance of

hypermethylated neuronal signaling pathways in the high BPA vs. control comparison, including

histamine H1 and H2 receptor mediated signaling, 5HT1 and 5HT4 serotonin receptor mediated

signaling pathways, β_1, β_2, and β_3 adrenergic receptor signaling pathways, thyrotropin-releasing

hormone receptor signaling, GABA and glutamate receptor signaling, and muscarinic

acetylcholine receptor 1, 2, 3 and 4 signaling (**Table 4.4**). Non-neuronal pathways significant in

the high BPA vs. control comparison include Erk signaling (*role of Erk5 in neuronal survival*,

p=1.8E-4, FDR=0.026) and PI3K signaling (*PI3 kinase pathway*, p=0.010, FDR=0.047)

pathways (**Table 4.4**). Two pathway terms were significant in the low BPA vs. control

comparison, including *selenocompound metabolism* (p=1.3E-5, FDR=.0026), which may be linked to cellular redox state (**Table 4.4**).

The pathways were further analyzed using a hypothesis-driven approach for relevance to human exposure to BPA and to the HCC phenotype under study. Jak/Stat and Mapk signaling have previously been implicated in the literature in mediating estrogen-dependent male:female incidence not seen in the liver tumor phenotype described in Chapter 2 (Sekine et al., 2004, Shi et al., 2014a). Hypothesis-driven analysis revealed 70 mouse microarray gene IDs in selected concepts related to Jak/Stat and 110 related to Mapk across all four dose comparisons. Sixty-one genes within human JAK/STAT and 177 genes within human MAPK signaling pathways known to be altered by BPA were compared to mouse microarray gene IDs. Mouse microarray results overlapped with human homologs with known interactions with BPA at 10 genes in JAK/STAT signaling (**Table 4.5, Figures 4.1** and **4.3**), including the kinase *JAK1* and the transcription factors *STAT5A* and *STAT5B*, and at 32 genes in MAPK signaling (**Table 4.6, Figures 4.2** and **4.4),** including the oncogene *MYC* and ten members of the *mitogen-activated kinase* (*MAP kinase*) family.

4.5   Discussion

Previously, we reported a dose-dependent increase in hepatic tumors in mice exposed during gestation and lactation, with exposure cessation at weaning, to one of three doses of the endocrine disruptor BPA via maternal diet (50 ng, 50 µg, or 50 mg BPA/kg maternal diet, or phytoestrogen-free control diet). To our knowledge, the referenced study represented the first report of frank tumors following exposure to BPA alone, with no chemical or hormonal promoters of disease formation, in early life or in adulthood. Observed hepatic tumors showed early onset of disease at 10 months of age, rather than 12 months or older, and did not display

classical sexual dimorphism in incidence, suggesting a distinct disease etiology. The last formal evaluation of the potential carcinogenicity of BPA in the United States was performed in 1982 by the National Toxicology Program, which found no compelling evidence of carcinogenicity following exposure of adult mice and rats to doses ranging from 200-20,000 times as high as the doses employed in our study, underscoring the importance of early life exposure testing.

The promoter tiling DNA methylation microarrays employed in the present study provides a useful tool for assessing potential epigenome-wide methylation changes at nearly every promoter in the mouse genome. Tiling along promoter regions and use of enrichment arrays, allow for detection of regions of altered DNA methylation. As demonstrated in Chapter 3, even adjacent CpG sites may exhibit different levels of basal methylation and lability following environmental exposures, supporting the use of methods that detect larger regions of DNA methylation patterning.

Although we did not identify many individual probes with FDR<0.1, gene set enrichment testing revealed to be a powerful approach to detect subtle but consistent changes across a GO term or pathway. The lack of significant individual probes may be due to the small sample sizes, and higher than anticipated variability. However, the relative proportion of probes with p-value<0.1 for animals with liver tumors versus without liver tumors indicates notable patterns of change that suggest specific biological responses and provide direction for future work; approximately 1.8% of probes (almost twice the expected 1%) were differentially methylated in animals with liver tumors as compared to animals without tumors, 67.5% of which were hypomethylated. Mice exposed to high dose BPA were differentially methylated at 1.3% of probes as compared to control mice, 67% of which were hypomethylated. However, 65% of differentially methylated probes in mice exposed to high dose BPA as compared to mice exposed

to low dose BPA showed an increase in methylation, suggesting a lack of a linear increase or decrease in overall promoter DNA methylation levels with increasing BPA exposure.

GO term enrichment yielded several terms indicating altered epigenetic patterning across the epigenome, supporting the hypothesis of large scale, yet subtle, epigenomic change in mice following BPA exposure, as well as in cancer phenotypes. The GO Term *selenocompound metabolism,* which was significantly enriched for in animals exposed to low BPA versus control animals, may be associated with biotransformation, which involves a class of selenoenzymes such as glutathione peroxidase, and cellular proliferation (Erkekoglu et al., 2014). Animals with liver tumors showed enrichment for genes in the one-carbon metabolic process GO term as compared to animals without liver tumors. This GO term included mitochondrial *serine hydroxymethyltransferase 2* (*Shmt2*) and *methionine adenosyltransferase I α* (*Mat1a*), which are linked not only to regulation of epigenetic patterning but also to liver function and pathology (Liu et al., 2007; Rountree et al., 2008). *Shmt2*-deficient mice develop chronic hepatitis and glycogen storage disease in the liver (Liu et al., 2007), and *Mat1a*-deficient mice exhibit expansion of liver cancer stem cells with aging and spontaneously develop HCC by 18 months (Rountree et al., 2008). Morphogenic and developmental processes, which were significantly enriched for in mice with tumors as compared to mice without tumors, may be altered due to cancer-related pathway reversion to embryonic states (Hanahan and Weinberg, 2011) or to a relative increase in the proportion of stem cells in liver tissue, suggested by a dose-dependent increase in oval cell hyperplasia noted in mice with hepatic tumors (Weinhouse et al., 2014).

Agnostic analysis of pathway terms with FDR<0.1 revealed a predominance of hypermethylated neuronal pathways, including histamine receptor signaling, serotonin receptor signaling, β-adrenergic receptor signaling, and thyrotropin releasing hormone receptor signaling.

Interestingly, several of these neuronal signaling pathways are linked to energy regulation and metabolic function, suggesting that BPA-induced disruption of neuronal signaling pathways may have metabolic consequences in the liver. Metabolic dysfunction is a common risk factor for both HCC (Lukanova et al., 2014) and HA (Farges & Dokmak, 2010). Histamine receptor signaling has been implicated in glucose and lipid metabolism and plays a role in the development of hyperlipidemia-induced non-alcoholic steatohepatitis (NASH) (Wang et al., 2010). Endogenous histamine levels can reduce plasma IGF-1 levels, necessary for growth and development, via histamine 1 receptor (H1R) signaling in rats (Liao et al., 2001). Histamine (Knigge et al., 1984) and serotonin (Castrogiovanni et al., 2014) also regulate growth hormone secretion, which in turn stimulates hepatic production of IGF-1. Increased serotonin levels lead to limited differentiation and development (Castrogiovanni et al., 2014) as well as hypoglycemia (Endo 1991). Signaling via β-adrenergic receptors has been reported to drive lipolysis in adipose tissue (Thompson et al., 2014), suggesting that suppression of these pathways is consistent with lipid accumulation, or steatosis, observed in study animals in Chapter 2. Thyroid hormone receptor signaling cross-talks with the adrenergic nervous system in the liver to modulate insulin sensitivity and suppression of hepatic gluconeogenesis (Mullur et al., 2014). These results also suggest the proliferative response observed in Chapter 2. Growth factors linked to histamine and serotonin receptor signaling, including IGF-1 and growth hormone, promote cellular proliferation and angiogenesis and repress apoptosis (Castrogiovanni et al., 2014; Knigge et al., 1984; Liao et al., 2001).

Hypothetically, suppression of these neuronal pathways suggested by the observed promoter DNA hypermethylation response would allow for higher tissue levels of Igf1 and increased proliferative response in the liver. However, these results should be interpreted with

132

caution, as none of the 19 pathway terms related to IGF signaling, insulin signaling, or growth hormone signaling were statistically enriched for in these analyses. In addition, neuronal signaling pathways identified here may be related to phenotypic effects of BPA exposure other than liver tumors. Perinatal BPA exposure has been linked to hyperactivity and anxiety (Anderson et al., 2013), behaviors than have been linked to decreased serotonin levels and signaling in the hippocampus (Texel et al., 2012).

In addition to our agnostic results, we chose to analyze these microarray data with a hypothesis-driven approach. The classical sexual dimorphism in incidence not seen in our study is well accepted to result from a suppression of IL-6 production by endogenous estradiol and downstream suppression of STAT3 signaling (Sekine et al., 2004). BPA has been shown to induce IL-6 expression directly in HepG2 cells, a human HCC cell line (Moon et al., 2012), and to increase expression of both STAT3 and ELK-1, a MAPK pathway indicator, in human hepatoma Hep3b cells (Sekine et al., 2004). As Jak/Stat and Mapk signaling pathways have previously been implicated in male: female dimorphism in incidence notably absent in our observed tumors, we chose to investigate a potential link between these pathways and hepatic tumors in BPA-exposed mice. We report an overlap of genes implicated in Jak/STAT and MAPK signaling with altered 5' promoter methylation in mice perinatally exposed to BPA presenting with hepatic tumors, with genes linked to the same pathways noted to respond to human BPA exposure in The Comparative Toxicogenomics Database (Davis et al., 2014). Three key overlapping genes, *Jak1*, *Stat5b*, and *Akt1*, have previously characterized roles linked to liver carcinogenesis.

JAK1 activation mediates PI3K and Akt phosphorylation and contribute to downstream inflammation in immortalized human HSC (LX-2) cells and in human HCC (HepG2) cells (Niu

et al., 2007). STAT5b activation is associated with epithelial-to-mesenchymal transition in human clinical HCC samples, and is linked to younger age and advanced tumor stages (Lee et al., 2006). STAT5b is also required for differential liver gene expression, due to its role in signal transduction for a number of cytokines and growth factors, including growth hormone (Udy et al., 1997). The male pattern of pulsatile growth hormone secretion, as opposed to the female pattern of continuous secretion, is stimulated in the neonatal period by gonadal steroids (Ramirez et al., 2012) and activates liver STAT5b to stimulate transcription of STAT, which regulates sexual dimorphism of liver gene expression (Udy et al., 1997). Therefore, STAT5b gene disruption leads to a loss of multiple sexually differentiated responses (Udy et al., 1997). Female rats exposed to 50 or 500 µg BPA from post-natal day 1 to post-natal day 10 showed increased levels of pituitary growth hormone and liver IGF-1 at 5 months of age, as well as downregulation of female-predominant liver enzyme Cyp2c12, with no changes in male predominant Cyp2c11 (Ramirez et al., 2012). These data suggest that perinatal BPA exposure may diminish sexual dimorphism in liver gene expression via altered growth hormone signaling, perhaps regulated by STAT5b.

Interestingly, BPA exposure did not increase risk for hepatic tumors in male mice as compared to female mice in Chapter 2, and higher endogenous levels of estradiol did not mitigate the effects of BPA exposure in female mice, suggesting an estrogen-independent mechanism for tumorigenesis. Although loss of estradiol-mediated protection in females due to competitive binding of BPA to ERα is unlikely due to estradiol's greater affinity for canonical estrogen receptors (Alonso-Magdalena et al., 2012), BPA may directly activate downstream STAT3 signaling by binding to IL-6 receptor or related receptors with a shared gp130 intracellular signaling domain, such as leptin receptor. Gestational exposure to BPA in rodents

has alternately been demonstrated to increase serum leptin in male CD-1 mice (Angle et al., 2013), to decrease serum leptin in female C57BL/6JxFVB hybrid mice (van Esterik et al., 2014), or to induce no change in a/a mice derived from the A^{vy} strain (genetically 93% C57BL/6J) (Anderson et al., 2013, Weinhouse et al., 2014). However, BPA induced leptin receptor expression and downstream activation of Jak/STAT, MAPK/ERK, and PI3K/Akt pathways in human OVCAR-3 ovarian cancer cells (Ptak et al., 2014). Serum BPA has been associated with circulating leptin levels in humans (Rönn et al., 2014).

Pathway terms identified via agnostic pathway analysis do support a potential role for Jak/Stat and Mapk mediated inflammation in hepatic tumorigenesis following BPA exposure. For example, PI3K and Erk signaling pathways were noted in the high BPA vs. control comparison (Table 4.3); both of these pathways crosstalk with Jak/Stat and Mapk signaling and both have been implicated in BPA exposure in rodents (Ptak et al., 2014). Further, inflammatory and neuronal signaling pathways, identified via hypothesis-driven and agnostic analyses, respectively, may crosstalk with respect to the observed phenotype, as well. Macrophages produce cytokines in response to inflammation that increase liver serotonin, leading to hypoglycemia (Endo, 1991) Serotonin regulates inflammation and tissue repair and contributes to the maintenance of an anti-inflammatory state via 5HT2 signaling (de las Casas-Engel et al., 2013).

This epigenome-wide promoter methylation tiling microarray platform is intended as a discovery tool for identification of large scale, pathway level changes linked to exposure and disease that demonstrate translational relevance of our observed liver tumor phenotype to guide future studies. This exploratory study has successfully characterized pathways and generated hypotheses for future work, as well as provided evidence for relevance to human health.

However, these results must be interpreted within the limitations of our experimental design and platform. These microarray experiments yielded qualitative, rather than quantitative, data, which were not fully quantitatively validated via bisulfite sequencing (**Table 4.2**). In addition, promoter DNA methylation measurement at a single time-point may not reflect alterations in all epigenomic markers over the life-course of exposed animals. Of note, highly networked pathways, such as Jak/Stat and Mapk signaling pathways, cannot themselves serve as biomarkers. Rather, once implicated, the roles of individual genes within these pathways and phenotypic evidence for functional change resulting from pathway activation or suppression, must be thoroughly investigated for their potential roles in hepatic tumor development following perinatal BPA exposure. Further, these results should be interpreted cautiously in a functional context. Although presence and directionality of 5' gene promoter methylation change often correlates negatively with transcriptional activity, prior studies have demonstrated a lack of concordance in matched experimental methylation and transcriptional datasets (Dhimolea et al., 2014), which may be due to residual methylation changes following a prior, undetected transcriptional change, or may indicate a lack of associated transcriptional change.

Future studies will need to carefully consider the relative roles of individual genes within pathways, overall pathway activation or suppression, and direction of change (hypomethylation or hypermethylation of 5' promoter regions) of individual and groups of genes. The direction of change is difficult to determine in the context of this study, as pathway databases used in pathway enrichment include several overlapping pathway terms that may include some or all of the genes in a pathway of interest. For example, pathway terms for both JAK/STAT and MAPK pathways were alternately noted as hypomethylated or hypermethylated following pathway enrichment. Further, genes implicated by each pathway term may individually be

hypomethylated or hypermethylated at their respective 5' promoter regions. Additionally, as previously reported, mononuclear inflammation was evident on histopathological evaluation in approximately 50% of study animals (Weinhouse et al., 2014). Incidence or severity of inflammation did not differ by dose group, tumor status, or sex (Weinhouse et al., 2014). Corn oil was substituted for soybean oil in phytoestrogen-free control diet, which was fed to all study animals following cessation of BPA exposure at weaning. Corn oil is rich in ω-6 fatty acids, which may induce an inflammatory response; however, corn oil-rich diets have been shown to decrease age-related inflammation and related markers, including IL-6, in livers of C57BL/6J mice (Si et al., 2014). Remaining variables shared among all study mice including genetic background and age. As our mouse strain is relatively resistant to HCC (Weinhouse et al., 2014), we hypothesize that inflammation noted in 10-month mice in this study is primarily due to age. Although visible dose- and tumor-dependent inflammation would be expected to accompany Jak/STAT and MAPK pathway activation, we cannot rule out the possibility of transient low level inflammation due to chronic early life BPA exposure, or, alternatively, persistent low grade inflammation masked by later age-related responses. Future studies that include observation of animals at earlier time points prior to tumor development would clarify temporality of inflammation and its potential link with perinatal BPA exposure.

4.6   Conclusion

Here, we investigate epigenome-wide changes in promoter DNA methylation in mice with hepatic tumors perinatally exposed to BPA. Our results suggest broad-scale, yet small magnitude, changes in DNA methylation due to BPA exposure and/or by tumor status. This is concluded based on the lack of a considerable number of individual probes with significant FDR values, together with the observation of many significant GO term and pathway results,

including several having known links with the effects of BPA. Several neuronal pathways

exhibited a hypermethylation response, which may be linked to metabolic dysfunction and

increased cellular proliferation in the liver. Genes in Jak/Stat and Mapk pathways linked to a lack

of characteristic sexual dimorphism in a hepatic tumor phenotype relevant to mice and humans

are also implicated in BPA exposure in the same pathways in humans, supporting involvement of

these pathways in both human BPA exposure and human HCC. Taken together, these findings

are significant indicators of the relevance of the hepatic tumor phenotype seen in BPA-exposed

mice to human health. This work demonstrates that epigenome-wide discovery experiments in

animal models are effective tools for identification and understanding of paralagous epimutations

salient to human disease.

4.7   References

Acevedo, N., Davis, B., Schaeberle, C. M., Sonnenschein, C., & Soto, A. M. (2013). Perinatally administered bisphenol a as a potential mammary gland carcinogen in rats. *Environmental Health Perspectives*, *121*(9), 1040–6.

Adriaens, M. E., Jaillard, M., Eijssen, L. M. T., Mayer, C.-D., & Evelo, C. T. A. (2012). An evaluation of two-channel ChIP-on-chip and DNA methylation microarray normalization strategies. *BMC Genomics*, *13*, 42.

Alonso-Magdalena, P., Ropero, A. B., Soriano, S., García-Arévalo, M., Ripoll, C., Fuentes, E., … Nadal, Á. (2012). Bisphenol-A acts as a potent estrogen via non-classical estrogen triggered pathways. *Molecular and Cellular Endocrinology*, *355*(2), 201–7.

Anderson, O. S., Nahar, M. S., Faulk, C., Jones, T. R., Liao, C., Kannan, K., … Dolinoy, D. C. (2012a). Epigenetic responses following maternal dietary exposure to physiologically relevant levels of bisphenol A. *Environmental and Molecular Mutagenesis*.

Anderson, O. S., Nahar, M. S., Faulk, C., Jones, T. R., Liao, C., Kannan, K., … Dolinoy, D. C. (2012b). Epigenetic responses following maternal dietary exposure to physiologically relevant levels of bisphenol A. *Environmental and Molecular Mutagenesis*.

Anderson, O. S., Peterson, K. E., Sanchez, B. N., Zhang, Z., Mancuso, P., & Dolinoy, D. C. (2013). Perinatal bisphenol A exposure promotes hyperactivity, lean body composition, and hormonal responses across the murine life course. *FASEB Journal : Official Publication of the Federation of American Societies for Experimental Biology*.

Angle, B. M., Do, R. P., Ponzi, D., Stahlhut, R. W., Drury, B. E., Nagel, S. C., … Taylor, J. A. (2013). Metabolic disruption in male mice due to fetal exposure to low but not high doses of bisphenol A (BPA): evidence for effects on body weight, food intake, adipocytes, leptin,

adiponectin, insulin and glucose regulation. *Reproductive Toxicology (Elmsford, N.Y.)*, *42*, 256–68.

Ashburner, M., Ball, C. A., Blake, J. A., Botstein, D., Butler, H., Cherry, J. M., … Sherlock, G. (2000). Gene ontology: tool for the unification of biology. The Gene Ontology Consortium. *Nature Genetics*, *25*(1), 25–9.

Avissar-Whiting, M., Veiga, K. R., Uhl, K. M., Maccani, M. A., Gagne, L. A., Moen, E. L., & Marsit, C. J. (2010). Bisphenol A exposure leads to specific microRNA alterations in placental cells. *Reproductive Toxicology (Elmsford, N.Y.)*, *29*(4), 401–6.

Baccarelli, A., & Bollati, V. (2009). Epigenetics and environmental chemicals. *Current Opinion in Pediatrics*, *21*(2), 243–51. ct

Bromer, J. G., Zhou, Y., Taylor, M. B., Doherty, L., & Taylor, H. S. (2010). Bisphenol-A exposure in utero leads to epigenetic alterations in the developmental programming of uterine estrogen response. *FASEB Journal : Official Publication of the Federation of American Societies for Experimental Biology*, *24*(7), 2273–80.

Calafat, A. M., Ye, X., Wong, L.-Y., Reidy, J. A., & Needham, L. L. (2008). Exposure of the U.S. population to bisphenol A and 4-tertiary-octylphenol: 2003-2004. *Environmental Health Perspectives*, *116*(1), 39–44.

Carcinogenesis Bioassay of Bisphenol A (CAS No. 80-05-7) in F344 Rats and B6C3F1 Mice (Feed Study). (1982). *National Toxicology Program Technical Report Series*, *215*, 1–116.

Castrogiovanni, P., Musumeci, G., Trovato, F. M., Avola, R., Magro, G., & Imbesi, R. (2014). Effects of high-tryptophan diet on pre- and postnatal development in rats: a morphological study. *European Journal of Nutrition*, *53*(1), 297–308.

Davis A.P., Grondin C. J., Lennon-Hopkins K., Saraceni-Richards C., Sciaky D., King B.L., Wiegers T.C., Mattingly C.J. (2014). The Comparative Toxicogenomics Database's 10th Year Anniversary: Update 2015. *Nucleic Acids Res*, 2014 Oct 17 Epub.

De las Casas-Engel, M., Domínguez-Soto, A., Sierra-Filardi, E., Bragado, R., Nieto, C., Puig-Kroger, A., … Corbí, A. L. (2013). Serotonin skews human macrophage polarization through HTR2B and HTR7. *Journal of Immunology (Baltimore, Md. : 1950)*, *190*(5), 2301–10.

Dhimolea, E., Wadia, P. R., Murray, T. J., Settles, M. L., Treitman, J. D., Sonnenschein, C., … Soto, A. M. (2014). Prenatal exposure to BPA alters the epigenome of the rat mammary gland and increases the propensity to neoplastic development. *PloS One*, *9*(7), e99800.

Doherty, L. F., Bromer, J. G., Zhou, Y., Aldad, T. S., & Taylor, H. S. (2010). In utero exposure to diethylstilbestrol (DES) or bisphenol-A (BPA) increases EZH2 expression in the mammary gland: an epigenetic mechanism linking endocrine disruptors to breast cancer. *Hormones & Cancer*, *1*(3), 146–55.

Dolinoy, D. C., Huang, D., & Jirtle, R. L. (2007). Maternal nutrient supplementation counteracts bisphenol A-induced DNA hypomethylation in early development. *Proceedings of the National Academy of Sciences of the United States of America*, *104*(32), 13056–61.

Dolinoy, D. C., & Jirtle, R. L. (2008). Environmental epigenomics in human health and disease. *Environmental and Molecular Mutagenesis*, *49*(1), 4–8.

Doshi, T., Mehta, S. S., Dighe, V., Balasinor, N., & Vanage, G. (2011). Hypermethylation of estrogen receptor promoter region in adult testis of rats exposed neonatally to bisphenol A. *Toxicology*, *289*(2-3), 74–82.

Endo, Y. (1991). Parallel relationship between the increase in serotonin in the liver and the hypoglycaemia induced in mice by interleukin-1 and tumour necrosis factor. *Immunology Letters*, *27*(1), 75–9.

Erkekoglu, P., Zeybek, N. D., Giray, B. K., Rachidi, W., Kızılgün, M., Hininger-Favier, I., … Hincal, F. (2014). The effects of di(2-ethylhexyl)phthalate on rat liver in relation to selenium status. *International Journal of Experimental Pathology*, *95*(1), 64–77.

Farges, O., & Dokmak, S. (2010). Malignant transformation of liver adenoma: an analysis of the literature. *Digestive Surgery*, *27*(1), 32–8.

Greathouse, K. L., Bredfeldt, T., Everitt, J. I., Lin, K., Berry, T., Kannan, K., … Walker, C. L. (2012). Environmental Estrogens Differentially Engage the Histone Methyltransferase EZH2 to Increase Risk of Uterine Tumorigenesis. *Molecular Cancer Research : MCR*, *10*(4), 546–57.

Hanahan, D., & Weinberg, R. A. (2011). Hallmarks of cancer: the next generation. *Cell*, *144*(5), 646–74.

Huber, W., von Heydebreck, A., Sültmann, H., Poustka, A., & Vingron, M. (2002). Variance stabilization applied to microarray data calibration and to the quantification of differential expression. *Bioinformatics (Oxford, England)*, *18 Suppl 1*, S96–104.

Kim, J. H., Sartor, M. A., Rozek, L. S., Faulk, C., Anderson, O. S., Jones, T. R., … Dolinoy, D. C. (2014). Perinatal bisphenol A exposure promotes dose-dependent alterations of the mouse methylome. *BMC Genomics*, *15*, 30.

Knigge, U., Thuesen, B., Wollesen, F., Dejgaard, A., & Christiansen, P. M. (1984). Histamine-induced paradoxical growth hormone response to thyrotropin-releasing hormone in normal men. *The Journal of Clinical Endocrinology and Metabolism*, *58*(4), 692–7.

Laird, P. W. (2010). Principles and challenges of genomewide DNA methylation analysis. *Nature Reviews. Genetics*, *11*(3), 191–203.

Liao, D. J., Blanck, A., Eneroth, P., Gustafsson, J. A., & Hällström, I. P. (2001). Diethylnitrosamine causes pituitary damage, disturbs hormone levels, and reduces sexual dimorphism of certain liver functions in the rat. *Environmental Health Perspectives*, *109*(9), 943–7.

Liu, S.-P., Li, Y.-S., Chen, Y.-J., Chiang, E.-P., Li, A. F.-Y., Lee, Y.-H., … Chen, Y.-M. A. (2007). Glycine N-methyltransferase-/- mice develop chronic hepatitis and glycogen storage disease in the liver. *Hepatology (Baltimore, Md.)*, *46*(5), 1413–25.

Lukanova, A., Becker, S., Hüsing, A., Schock, H., Fedirko, V., Trepo, E., … Kaaks, R. (2014). Prediagnostic plasma testosterone, sex hormone-binding globulin, IGF-I and hepatocellular carcinoma: etiological factors or risk markers? *International Journal of Cancer. Journal International Du Cancer*, *134*(1), 164–73.

Moon, M. K., Kim, M. J., Jung, I. K., Koo, Y. Do, Ann, H. Y., Lee, K. J., … Park, Y. J. (2012). Bisphenol A impairs mitochondrial function in the liver at doses below the no observed adverse effect level. *Journal of Korean Medical Science*, *27*(6), 644–52.

Mullur, R., Liu, Y.-Y., & Brent, G. A. (2014). Thyroid hormone regulation of metabolism. *Physiological Reviews*, *94*(2), 355–82.

Niu, L., Wang, X., Li, J., Huang, Y., Yang, Z., Chen, F., … Cao, Q. (2007). Leptin stimulates alpha1(I) collagen expression in human hepatic stellate cells via the phosphatidylinositol 3-kinase/Akt signalling pathway. *Liver International : Official Journal of the International Association for the Study of the Liver*, *27*(9), 1265–72.

Prins, G. S., Hu, W.-Y., Shi, G.-B., Hu, D.-P., Majumdar, S., Li, G., … van Breemen, R. B. (2014). Bisphenol A promotes human prostate stem-progenitor cell self-renewal and increases in vivo carcinogenesis in human prostate epithelium. *Endocrinology*, *155*(3), 805–17.

Pupo, M., Pisano, A., Lappano, R., Santolla, M. F., De Francesco, E. M., Abonante, S., … Maggiolini, M. (2012). Bisphenol A Induces Gene Expression Changes and Proliferative Effects through GPER in Breast Cancer Cells and Cancer-Associated Fibroblasts. *Environmental Health Perspectives*.

Ramirez, M. C., Bourguignon, N. S., Bonaventura, M. M., Lux-Lantos, V., Libertun, C., & Becu-Villalobos, D. (2012). Neonatal xenoestrogen exposure alters growth hormone-dependent liver proteins and genes in adult female rats. *Toxicology Letters*, *213*(3), 325–31.

Reimers, M. (2010). Making informed choices about microarray data analysis. *PLoS Computational Biology*, *6*(5), e1000786.

Rönn, M., Lind, L., Örberg, J., Kullberg, J., Söderberg, S., Larsson, A., … Lind, P. M. (2014). Bisphenol A is related to circulating levels of adiponectin, leptin and ghrelin, but not to fat mass or fat distribution in humans. *Chemosphere*, *112*, 42–8.

Rountree, C. B., Senadheera, S., Mato, J. M., Crooks, G. M., & Lu, S. C. (2008). Expansion of liver cancer stem cells during aging in methionine adenosyltransferase 1A-deficient mice. *Hepatology (Baltimore, Md.)*, *47*(4), 1288–97.

Sartor, M. A., Leikauf, G. D., & Medvedovic, M. (2009). LRpath: a logistic regression approach for identifying enriched biological groups in gene expression data. *Bioinformatics (Oxford, England)*, *25*(2), 211–7.

Shi, L., Feng, Y., Lin, H., Ma, R., & Cai, X. (2014). Role of estrogen in hepatocellular carcinoma: is inflammation the key? *Journal of Translational Medicine*, *12*(1), 93.

Si, H., Zhang, L., Liu, S., LeRoith, T., & Virgous, C. (2014). High corn oil dietary intake improves health and longevity of aging mice. *Experimental Gerontology*, *58C*, 244–249. doi:10.1016/j.exger.2014.09.001

Smyth, G. K., & Speed, T. (2003). Normalization of cDNA microarray data. *Methods (San Diego, Calif.)*, *31*(4), 265–73.

Sun, S., Huang, Y.-W., Yan, P. S., Huang, T. H., & Lin, S. (2011). Preprocessing differential methylation hybridization microarray data. *BioData Mining*, *4*, 13.

Tang, W., Morey, L. M., Cheung, Y. Y., Birch, L., Prins, G. S., & Ho, S. (2012). Neonatal exposure to estradiol/bisphenol A alters promoter methylation and expression of Nsbp1 and Hpcal1 genes and transcriptional programs of Dnmt3a/b and Mbd2/4 in the rat prostate gland throughout life. *Endocrinology*, *153*(1), 42–55.

Texel, S. J., Camandola, S., Ladenheim, B., Rothman, S. M., Mughal, M. R., Unger, E. L., … Mattson, M. P. (2012). Ceruloplasmin deficiency results in an anxiety phenotype involving

deficits in hippocampal iron, serotonin, and BDNF. *Journal of Neurochemistry*, *120*(1), 125–34.

Thompson, N., Huber, K., Bedürftig, M., Hansen, K., Miles-Chan, J., & Breier, B. H. (2014). Metabolic programming of adipose tissue structure and function in male rat offspring by prenatal undernutrition. *Nutrition & Metabolism*, *11*(1), 50.

Udy, G. B., Towers, R. P., Snell, R. G., Wilkins, R. J., Park, S. H., Ram, P. A., … Davey, H. W. (1997). Requirement of STAT5b for sexual dimorphism of body growth rates and liver gene expression. *Proceedings of the National Academy of Sciences of the United States of America*, *94*(14), 7239–44.

Van Esterik, J. C. J., Dollé, M. E. T., Lamoree, M. H., van Leeuwen, S. P. J., Hamers, T., Legler, J., & van der Ven, L. T. M. (2014). Programming of metabolic effects in C57BL/6JxFVB mice by exposure to bisphenol A during gestation and lactation. *Toxicology*, *321*, 40–52.

Vandenberg, L. N., Chahoud, I., Heindel, J. J., Padmanabhan, V., Paumgartten, F. J. R., & Schoenfelder, G. (2012). Urinary, circulating, and tissue biomonitoring studies indicate widespread exposure to bisphenol A. *Ciência & Saúde Coletiva*, *17*(2), 407–34.

Wang, H., Li, J., Gao, Y., Xu, Y., Pan, Y., Tsuji, I., … Li, X.-M. (2010). Xeno-oestrogens and phyto-oestrogens are alternative ligands for the androgen receptor. *Asian Journal of Andrology*, *12*(4), 535–47.

Waterland, R. A., & Jirtle, R. L. (2003). Transposable elements: targets for early nutritional effects on epigenetic gene regulation. *Molecular and Cellular Biology*, *23*(15), 5293–300.

Weinhouse, C., Anderson, O. S., Bergin, I. L., Vandenbergh, D. J., Gyekis, J. P., Dingman, M. A., … Dolinoy, D. C. (2014). Dose-dependent incidence of hepatic tumors in adult mice following perinatal exposure to bisphenol A. *Environmental Health Perspectives*, *122*(5), 485–91.

Welshons, W. V, Nagel, S. C., & vom Saal, F. S. (2006). Large effects from small exposures. III. Endocrine mechanisms mediating effects of bisphenol A at levels of human exposure. *Endocrinology*, *147*(6 Suppl), S56–69.

Table 4.1 Primer sets for bisulfite sequencing

Assay	Forward Primer	Reverse Primer	Product Size	T_A	Number of CpG sites
Lce1m	5'-TTAGATTGTTGATGGTTGTTGTTGT-3'	5'-AATACCCTCCAACCTCTTCCTACTA-3'	457bp	57ºC	14
Shmt2	5'-TTGGGTGATTATAAGATTTTATTTAGG-3'	5'-AAAACTTTTCAAACAAAACTCTCCA-3'	484bp	57ºC	16
Foxp2	5'-ATTTTGGGGATTGTTAAGAAGTAGT-3'	5'-CCCAACTTTTTCCAAAAATAAAAAA-3'	487bp	54ºC	8
Ift46	5'-TGTTTTTGGGTTAGGAAATTTTTTT-3'	5'-TCTCATCTTCTCTTACCTTACTATCCTAAA-3'	236bp	48ºC	4

Table 4.2 Microarray validation using bisulfite sequencing

	Microarray			Bisulfite sequencing validation		
Gene	Comparison	β coefficient	*P*-value	Comparison	β coefficient	*P*-value
Lce1m	Tumor vs. Non-tumor	0.64	7.10E-06	Tumor vs. Non-tumor	0.010	0.77
				Low vs. Control	0.018	0.85
				High vs. Control	0.024	0.64
				High vs. Low	0.0060	0.39
Foxp2	Low vs. Control	0.38	4.60E-06	Tumor vs. Non-tumor	-0.0089	0.015
				Low vs. Control	-0.0059	0.59
				High vs. Control	0.0074	0.081
				High vs. Low	0.013	0.14
Ift46	High vs. Control	3.2	2.20E-05	Tumor vs. Non-tumor	-0.0048	0.61
				Low vs. Control	0.027	0.018
				High vs. Control	0.010	0.075
				High vs. Low	-0.017	0.42
Shmt2	High vs. Low	3.2	2.20E-07	Tumor vs. Non-tumor	0.00090	0.73
				Low vs. Control	-0.019	0.0028
				High vs. Control	-0.0056	0.073
				High vs. Low	0.013	0.26

Table 4.3 GO terms enriched for in methylation microarray analyses of BPA-exposed mice with hepatic tumors

Name	ConceptType	Comparison	#Genes	P-Value	FDR	Direction
middle ear morphogenesis	GO Biological Process	Tumor vs. No tumor	11	1.87E-08	4.64E-05	up
ear morphogenesis	GO Biological Process	Tumor vs. No tumor	51	8.84E-08	1.10E-04	up
embryonic organ morphogenesis	GO Biological Process	Tumor vs. No tumor	95	2.03E-07	1.68E-04	up
ear development	GO Biological Process	Tumor vs. No tumor	66	1.40E-06	8.69E-04	up
sensory organ development	GO Biological Process	Tumor vs. No tumor	169	2.20E-06	0.001091	up
embryonic organ development	GO Biological Process	Tumor vs. No tumor	142	6.39E-06	0.002641	up
hepaticobiliary system development	GO Biological Process	Tumor vs. No tumor	50	1.03E-05	0.003484	up
liver development	GO Biological Process	Tumor vs. No tumor	49	1.12E-05	0.003484	up
chordate embryonic development	GO Biological Process	Tumor vs. No tumor	248	4.52E-05	0.01126	up
embryo development ending in birth or egg hatching	GO Biological Process	Tumor vs. No tumor	250	4.54E-05	0.01126	up
inner ear morphogenesis	GO Biological Process	Tumor vs. No tumor	41	6.34E-05	0.014279	up
kidney development	GO Biological Process	Tumor vs. No tumor	62	1.58E-04	0.03268	up
brain development	GO Biological Process	Tumor vs. No tumor	205	1.76E-04	0.033418	up
demethylation	GO Biological Process	Tumor vs. No tumor	14	1.94E-04	0.033418	up
renal system development	GO Biological Process	Tumor vs. No tumor	65	2.02E-04	0.033418	up
covalent chromatin modification	GO Biological Process	Tumor vs. No tumor	116	2.46E-04	0.038055	up
metanephros development	GO Biological Process	Tumor vs. No tumor	21	2.65E-04	0.038651	up
histone modification	GO Biological Process	Tumor vs. No tumor	113	2.88E-04	0.039684	up
positive regulation of DNA repair	GO Biological Process	Tumor vs. No tumor	13	3.66E-04	0.046376	up
multicellular organism growth	GO Biological Process	Tumor vs. No tumor	44	3.77E-04	0.046376	up
organ morphogenesis	GO Biological Process	Tumor vs. No tumor	434	3.93E-04	0.046376	up
organ growth	GO Biological Process	Tumor vs. No tumor	40	4.12E-04	0.046376	up

positive regulation of cell-matrix adhesion	GO Biological Process	Tumor vs. No tumor	14	5.06E-04	0.054574	down
camera-type eye development	GO Biological Process	Tumor vs. No tumor	77	5.80E-04	0.059948	up
double-strand break repair	GO Biological Process	Tumor vs. No tumor	44	6.21E-04	0.061604	up
urogenital system development	GO Biological Process	Tumor vs. No tumor	91	7.21E-04	0.06416	up
regulation of the force of heart contraction	GO Biological Process	Tumor vs. No tumor	11	7.23E-04	0.06416	down
palate development	GO Biological Process	Tumor vs. No tumor	29	7.27E-04	0.06416	up
central nervous system neuron development	GO Biological Process	Tumor vs. No tumor	18	7.51E-04	0.06416	up
histone demethylase activity	GO Molecular Function	Tumor vs. No tumor	10	9.82E-05	0.039075	up
demethylase activity	GO Molecular Function	Tumor vs. No tumor	13	1.39E-04	0.039075	up
specific transcriptional repressor activity	GO Molecular Function	Tumor vs. No tumor	26	5.12E-04	0.07352	up
protein methyltransferase activity	GO Molecular Function	Tumor vs. No tumor	38	5.23E-04	0.07352	up
Golgi to plasma membrane transport	GO Biological Process	Low BPA vs. Control	10	1.23E-05	0.030447	up
macromolecule transmembrane transporter activity	GO Molecular Function	Low BPA vs. Control	10	1.45E-04	0.040759	up
protein transmembrane transporter activity	GO Molecular Function	Low BPA vs. Control	10	1.45E-04	0.040759	up
NADP or NADPH binding	GO Molecular Function	Low BPA vs. Control	26	5.28E-04	0.098975	down
extrinsic to membrane	GO Cellular Component	High BPA vs. Control	47	3.15E-05	0.006091	up
heterotrimeric G-protein complex	GO Cellular Component	High BPA vs. Control	10	3.27E-05	0.006091	up
extrinsic to plasma membrane	GO Cellular Component	High BPA vs. Control	26	3.25E-04	0.040366	up
acid-thiol ligase activity	GO Molecular Function	High BPA vs. Control	13	5.11E-05	0.028725	up
sequence-specific DNA binding	GO Molecular Function	High BPA vs. Control	424	1.53E-04	0.043107	up
sequence-specific DNA binding	GO Molecular Function	High BPA vs. Control	614	2.56E-04	0.04804	up

transcription factor activity						
ligase activity, forming carbon-sulfur bonds	GO Molecular Function	High BPA vs. Control	22	4.02E-04	0.056521	up
extrinsic to membrane	GO Cellular Component	High BPA vs. Low BPA	47	3.15E-05	0.006091	up
heterotrimeric G-protein complex	GO Cellular Component	High BPA vs. Low BPA	10	3.27E-05	0.006091	up
extrinsic to plasma membrane	GO Cellular Component	High BPA vs. Low BPA	26	3.25E-04	0.040366	up
acid-thiol ligase activity	GO Molecular Function	High BPA vs. Low BPA	13	5.11E-05	0.028725	up
sequence-specific DNA binding	GO Molecular Function	High BPA vs. Low BPA	424	1.53E-04	0.043107	up
sequence-specific DNA binding transcription factor activity	GO Molecular Function	High BPA vs. Low BPA	614	2.56E-04	0.04804	up
ligase activity, forming carbon-sulfur bonds	GO Molecular Function	High BPA vs. Low BPA	22	4.02E-04	0.056521	up

Table 4.4 Pathway terms enriched for in methylation microarray analyses of BPA-exposed mice with hepatic tumors

Name	ConceptType	Comparison	#Genes	P-Value	FDR	Direction
Acute Myocardial Infarction	Biocarta Pathway	Tumor vs. No tumor	14	6.24E-04	0.093603	up
Selenocompound metabolism	KEGG Pathway	Low BPA vs. Control	13	1.28E-05	0.00258	up
African trypanosomiasis	KEGG Pathway	Low BPA vs. Control	19	9.75E-04	0.098459	down
Role of Erk5 in Neuronal Survival	Biocarta Pathway	High BPA vs. Control	10	1.76E-04	0.026328	up
Histamine H2 receptor mediated signaling pathway	Panther Pathway	High BPA vs. Control	12	0.002505	0.039036	up
Beta3 adrenergic receptor signaling pathway	Panther Pathway	High BPA vs. Control	15	0.002672	0.039036	up
5HT4 type receptor mediated signaling pathway	Panther Pathway	High BPA vs. Control	16	0.002882	0.039036	up
Endogenous cannabinoid signaling	Panther Pathway	High BPA vs. Control	13	0.002974	0.039036	up
Cortocotropin releasing factor receptor signaling pathway	Panther Pathway	High BPA vs. Control	17	0.002982	0.039036	up
Heterotrimeric G-protein signaling pathway-rod outer segment phototransduction	Panther Pathway	High BPA vs. Control	19	0.003299	0.039036	up
5HT1 type receptor mediated signaling pathway	Panther Pathway	High BPA vs. Control	20	0.004139	0.039036	up
Beta1 adrenergic receptor signaling pathway	Panther Pathway	High BPA vs. Control	23	0.004662	0.039036	up
Beta2 adrenergic receptor signaling pathway	Panther Pathway	High BPA vs. Control	24	0.005096	0.039036	up
GABA-B receptor II signaling	Panther Pathway	High BPA vs. Control	18	0.005347	0.039036	up
Metabotropic glutamate receptor group II pathway	Panther Pathway	High BPA vs. Control	27	0.008168	0.047157	up
Histamine H1 receptor mediated signaling pathway	Panther Pathway	High BPA vs. Control	27	0.008371	0.047157	up
Oxytocin receptor mediated signaling pathway	Panther Pathway	High BPA vs. Control	35	0.009135	0.047157	up
Muscarinic acetylcholine receptor 1 and 3 signaling pathway	Panther Pathway	High BPA vs. Control	34	0.010031	0.047157	up
Metabotropic glutamate receptor group III	Panther Pathway	High BPA vs. Control	39	0.010058	0.047157	up

pathway						
PI3 kinase pathway	Panther Pathway	High BPA vs. Control	30	0.010336	0.047157	up
5HT2 type receptor mediated signaling pathway	Panther Pathway	High BPA vs. Control	37	0.011884	0.04919	up
Thyrotropin-releasing hormone receptor signaling pathway	Panther Pathway	High BPA vs. Control	36	0.012129	0.04919	up
Muscarinic acetylcholine receptor 2 and 4 signaling pathway	Panther Pathway	High BPA vs. Control	34	0.014209	0.054593	up